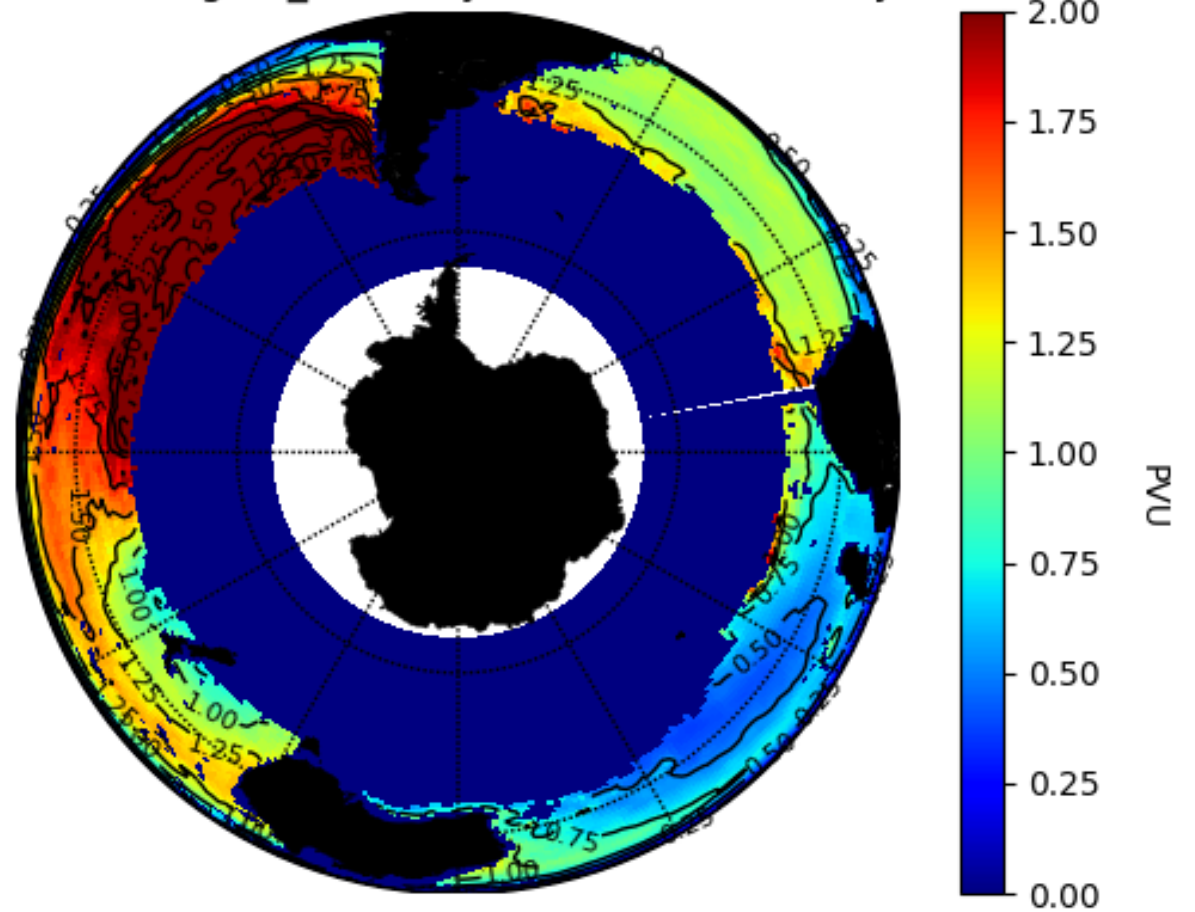


# Ocean-atmosphere coupling: theory and “observations”

Arnaud Czaja

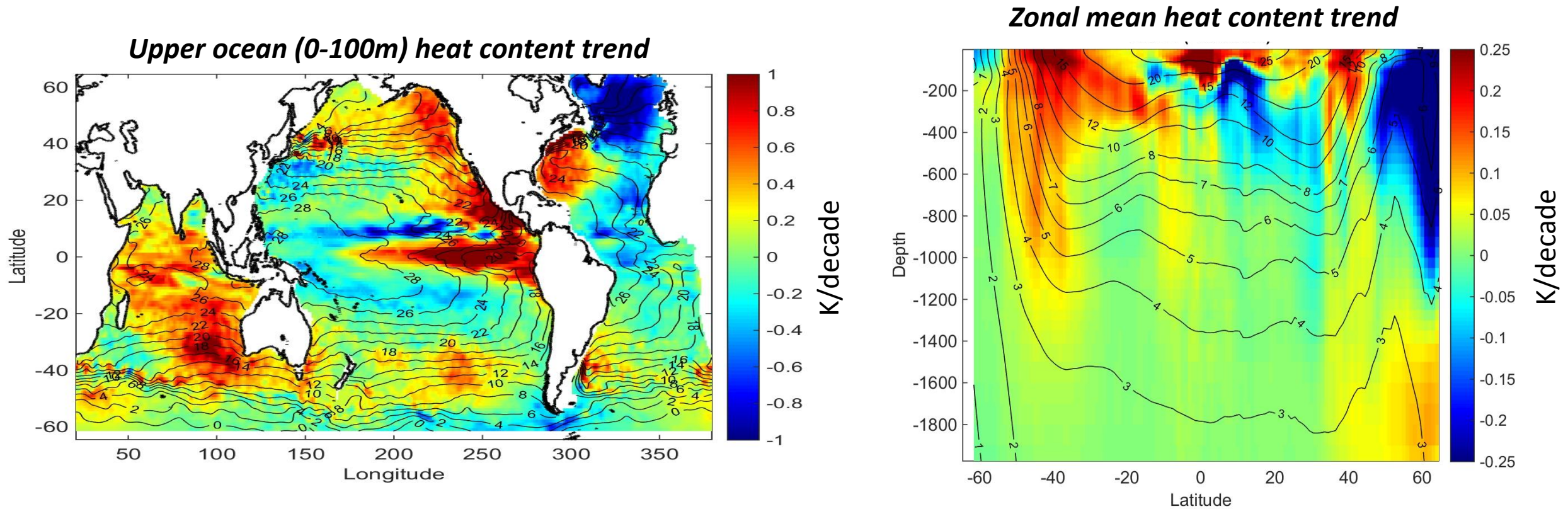
Imperial College London

PV on 26.6-26.8 sigma\_theta layer: ARGO mean for year 2016



- The rich dynamical behaviour of the ocean begins to be revealed by global observations

# Observed changes in ocean heat content from Argo floats (2004-2015)



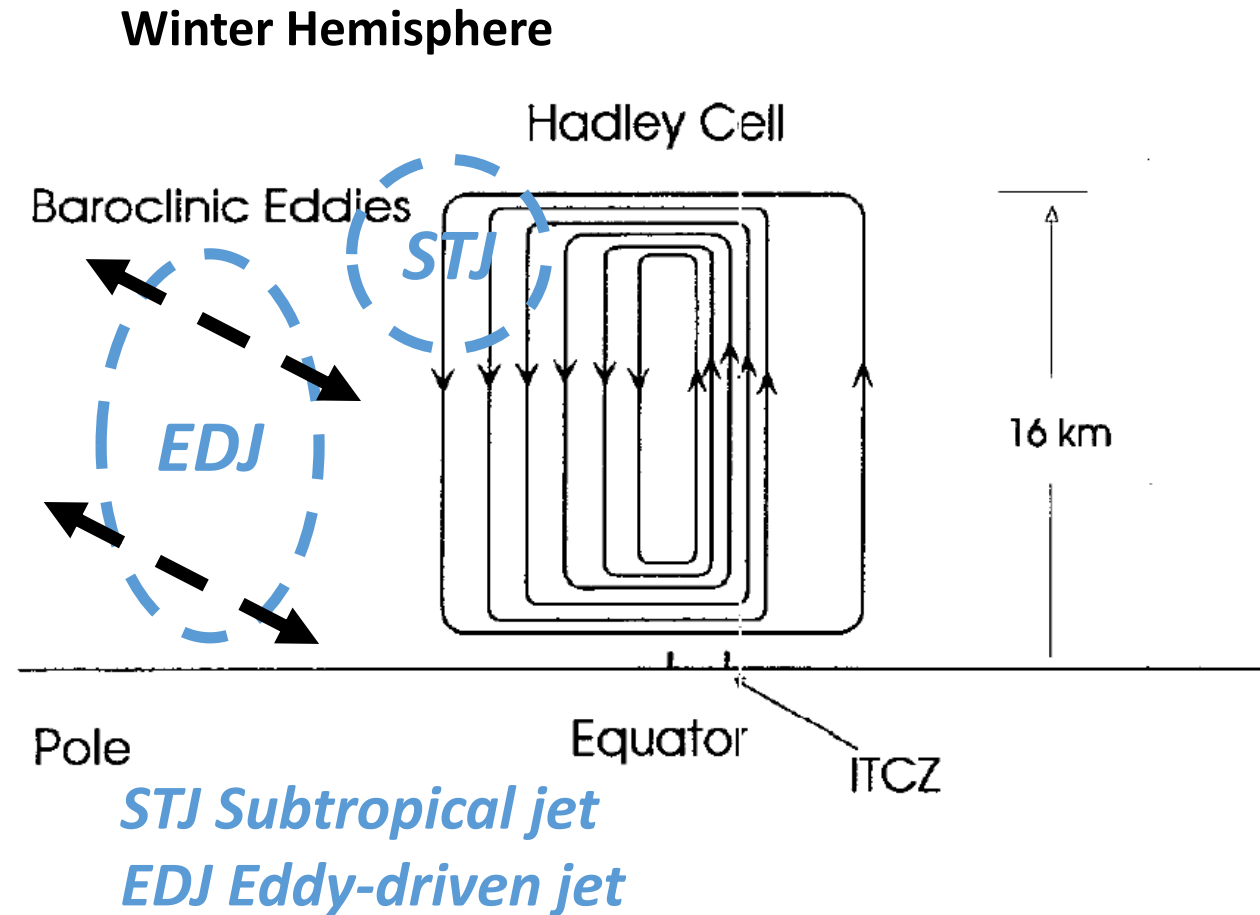
Global average  $\sim 0.5 \text{ W/m}^2$  driving sea level rise  $\sim 1\text{mm/yr}$ ...  
but also changes in global weather patterns?

# Key questions of this lecture:

- Are changes in upper ocean temperature only affecting the surface of the atmosphere (~1km)...?
- ...or do they extend upward beyond the first km or so?
- If so, how does it work?

# Key question of this lecture:

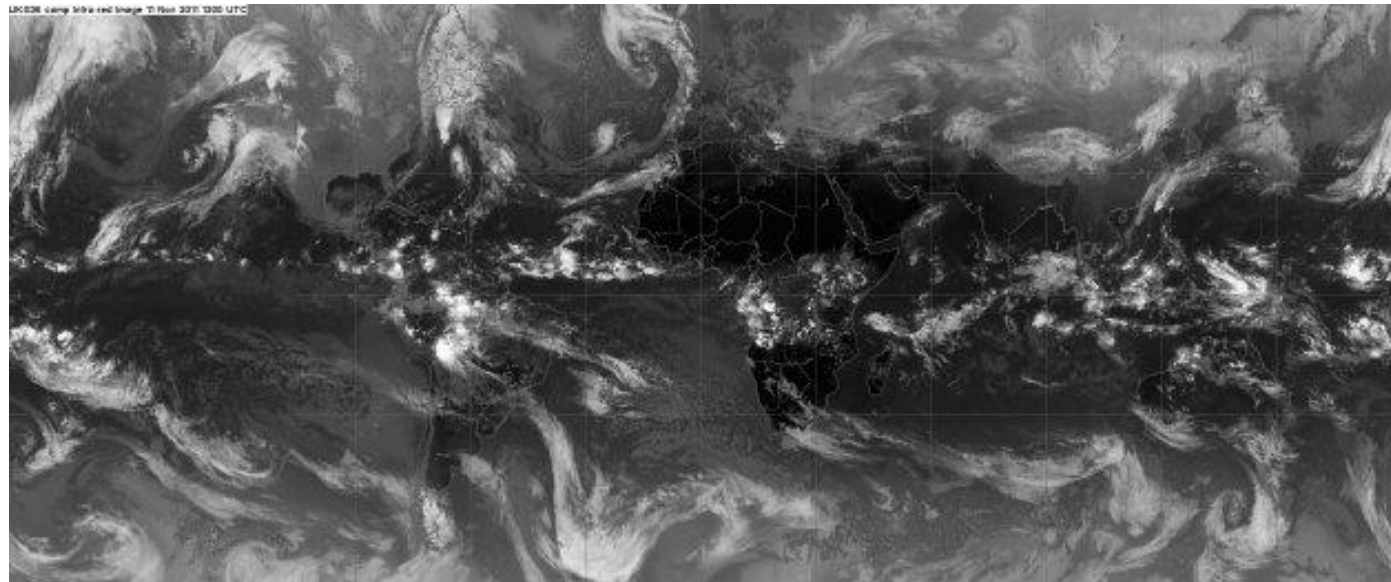
- Are changes in upper ocean temperature only affecting the surface of the atmosphere (~1km)...?
- ...or do they extend upward beyond the first km or so?
- If so, how does it work?



Picture adapted from Lindzen (1994)

# Outline

- An overview of observed “coupled variability” between oceans and atmosphere
- key issue: How do SST patterns affect the atmosphere above the boundary layer?

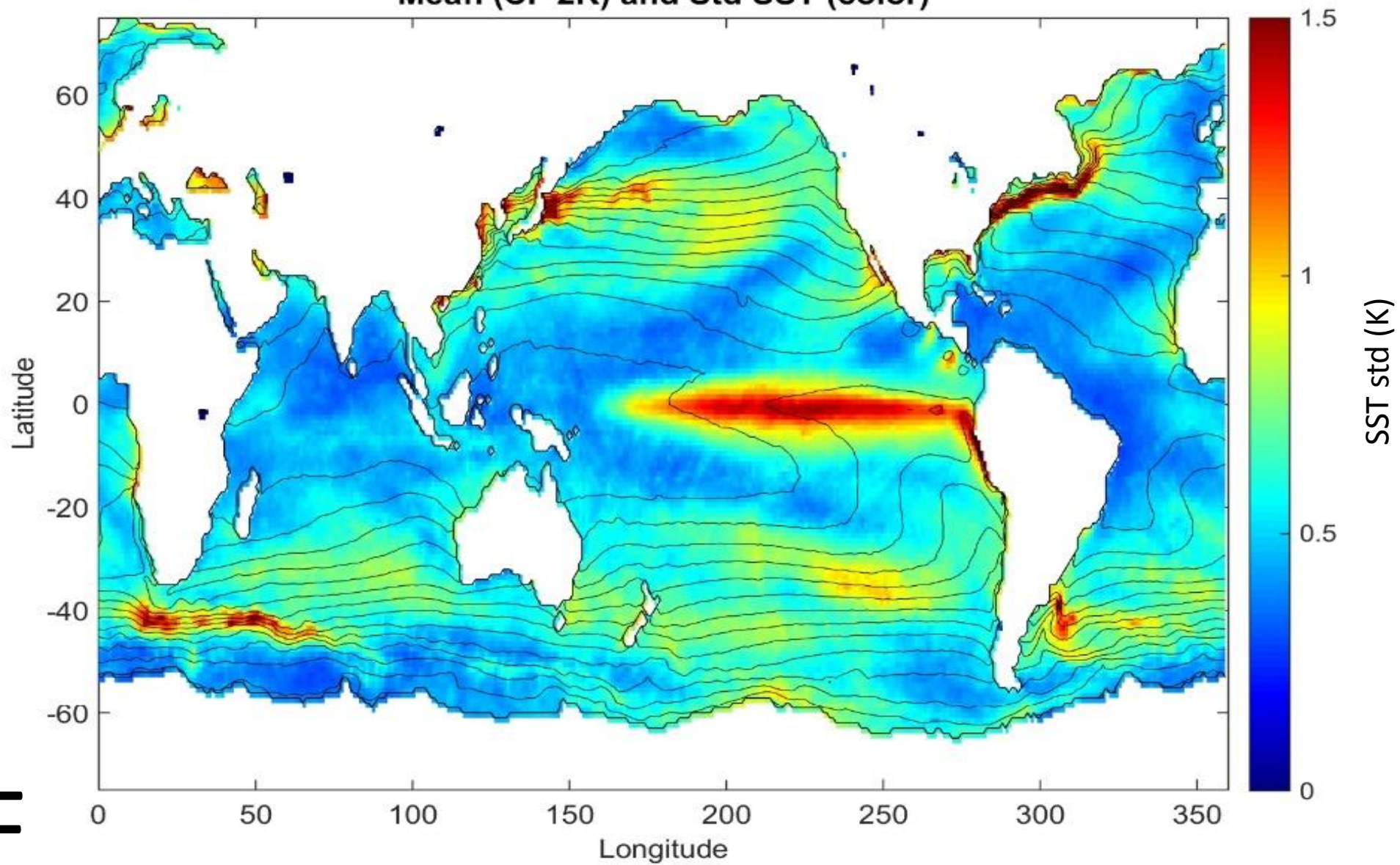


Infrared snapshot: white=cold=cloud top

# 1. An overview of “coupled” ocean-atmosphere variability

- Use de-seasonalised monthly anomalies in sea surface temperature (SST) and sea level pressure (SLP) to compare the observed variability in the North Atlantic, North Pacific, Equatorial Pacific and the Southern Ocean
- Apply a maximum covariance analysis (MCA) to SST and SLP from the ERA20C (1960-2010) reanalysis to do so
- Discuss predictability of ENSO and NAO

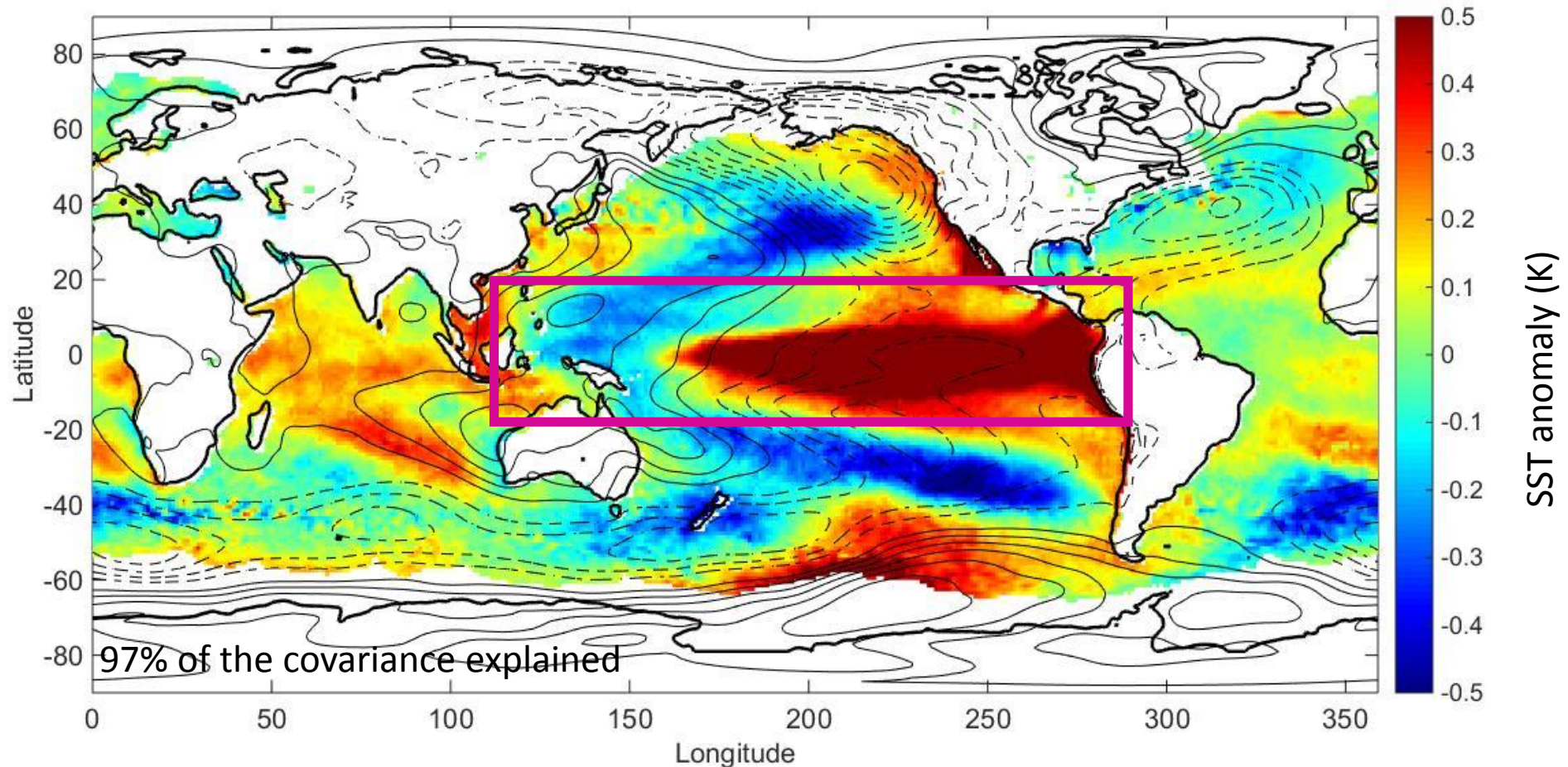
Mean (CI=2K) and Std SST (color)



DJF



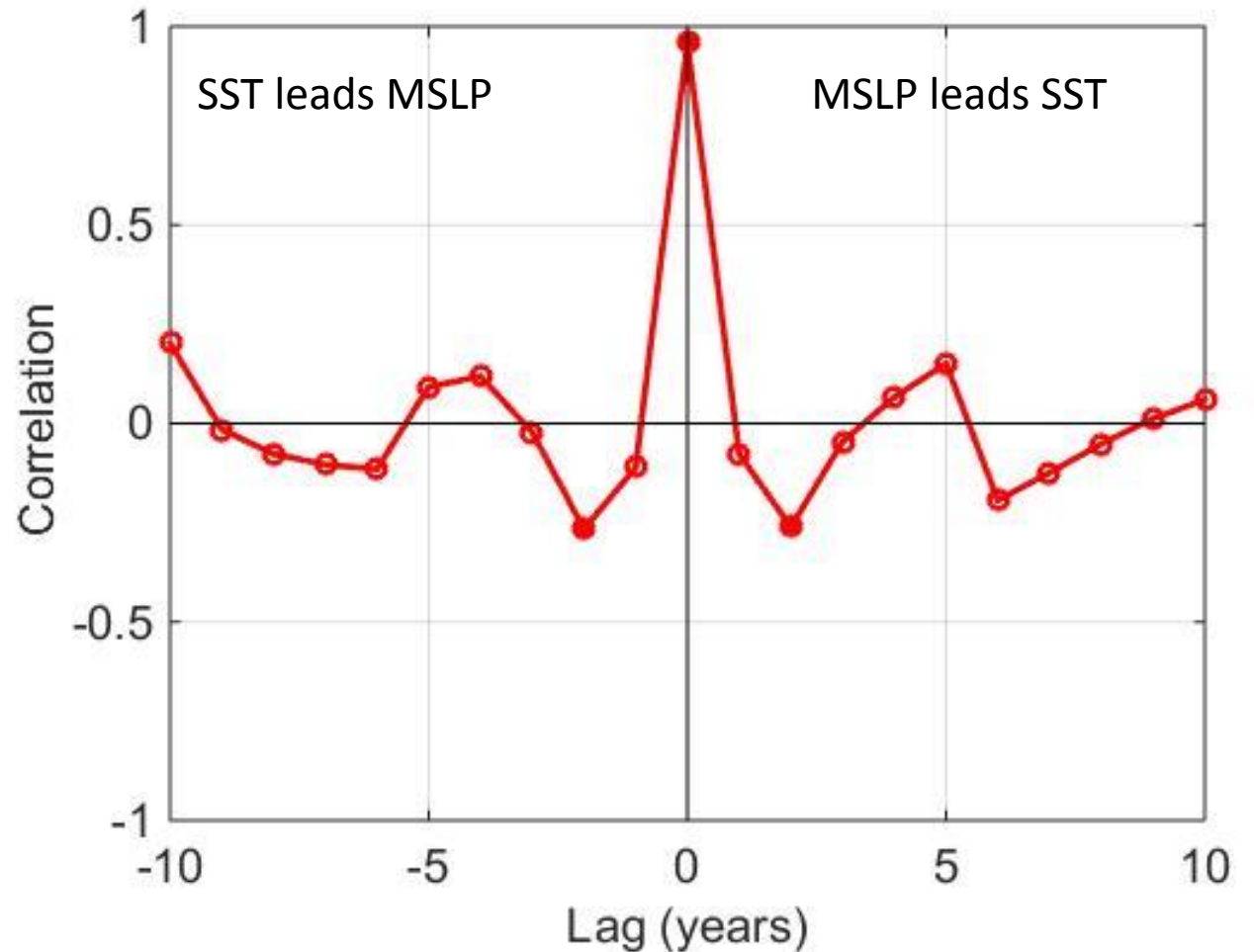
# SST (color) / MSLP (ci=0.25hPa) Equatorial Pacific (Max Cov. Ana., ERA20C, D-J-F 1960-2010)



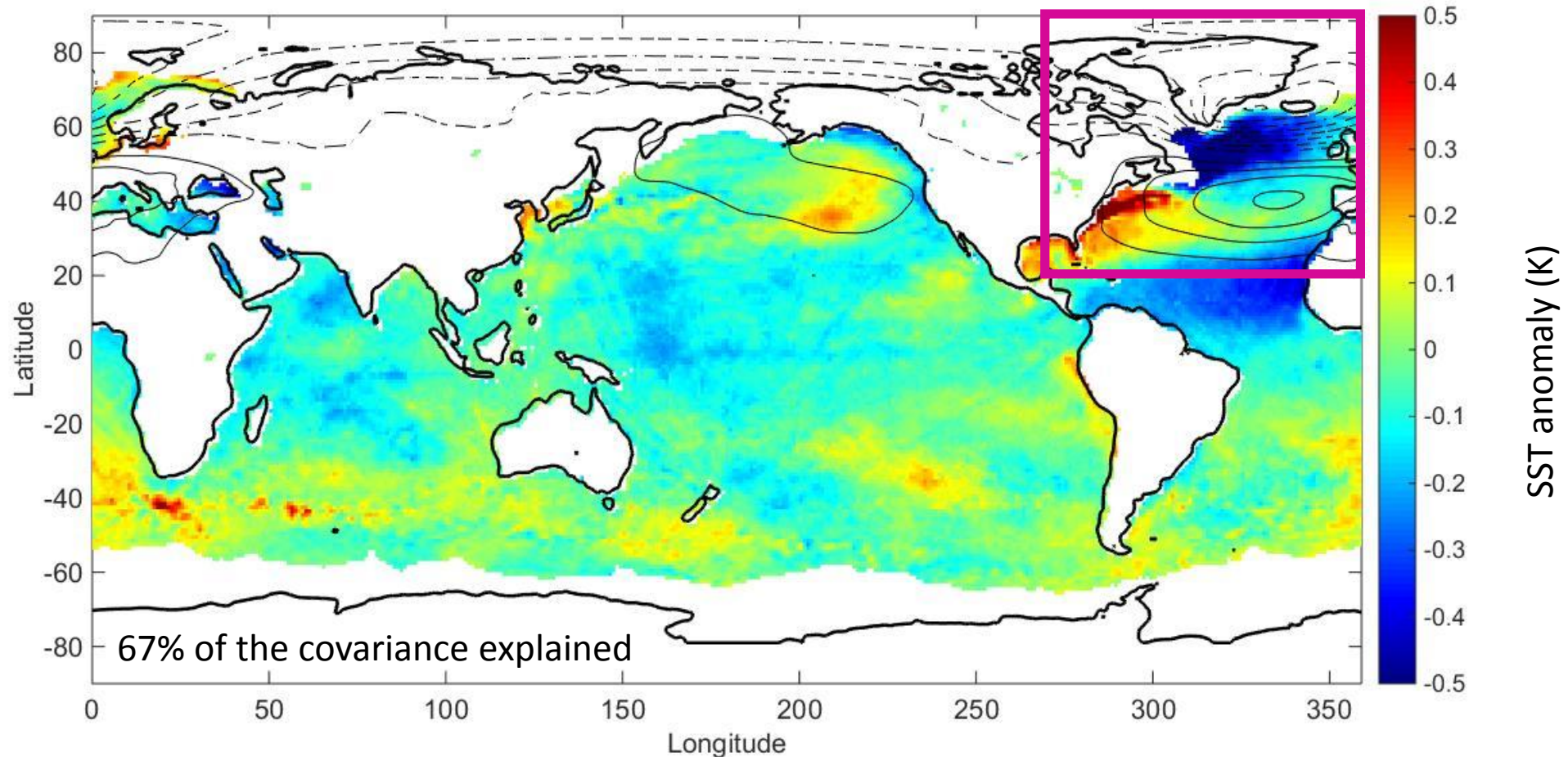
**NB** Analysis extended globally via linear regression

# SST / MSLP statistics for the Equatorial Pacific (Max Cov. Ana., ERA20C, D-J-F 1960-2010)

- Monthly statistics:  
SST 1-month autocor = 0.97  
MSLP 1-month autocor = 0.84  
Cross-corr: 0.89, 0.9, 0.89
- Longer timescale statistics:  
strong covariability, clear  
evidence of interannual  
oscillation



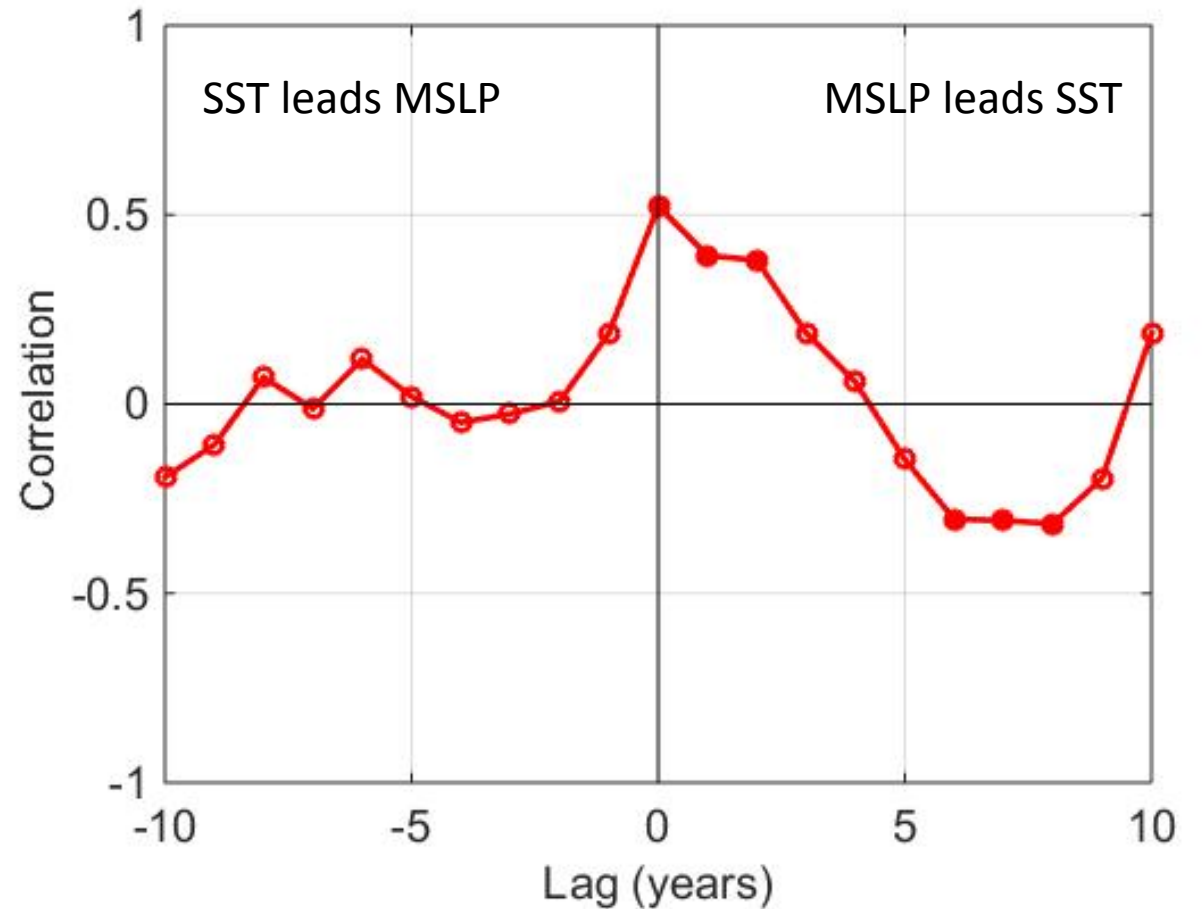
# SST (color) / MSLP (ci=1hPa) North Atlantic (Max Cov. Ana., ERA20C, D-J-F 1960-2010)



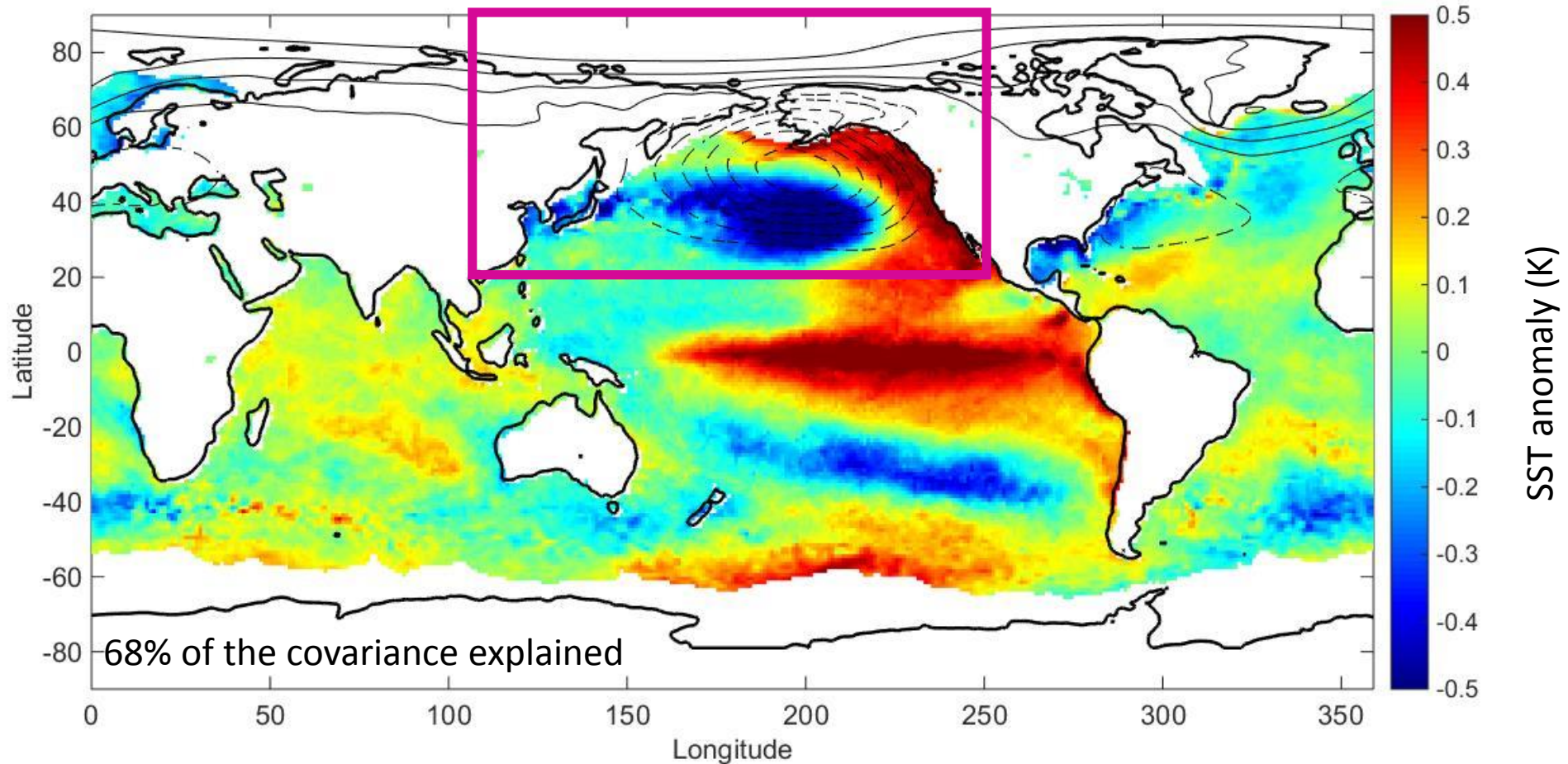
**NB** Analysis extended globally via linear regression

# SST / MSLP statistics for the North Atlantic (Max Cov. Ana., ERA20C, D-J-F 1960-2010)

- Monthly statistics:  
SST 1-month autocor = 0.86  
MSLP 1-month autocor = 0.24  
Cross-corr: 0.15, 0.47, 0.53
- Longer timescale statistics:  
indication of decadal oscillation,  
with SST pattern reversing sign  
6-8 years after MSLP



# SST (color) / MSLP (ci=1hPa) North Pacific (Max Cov. Ana., ERA20C, D-J-F 1960-2010)



**NB** Analysis extended globally via linear regression

# SST / MSLP statistics for the North Pacific (Max Cov. Ana., ERA20C, D-J-F 1960-2010)

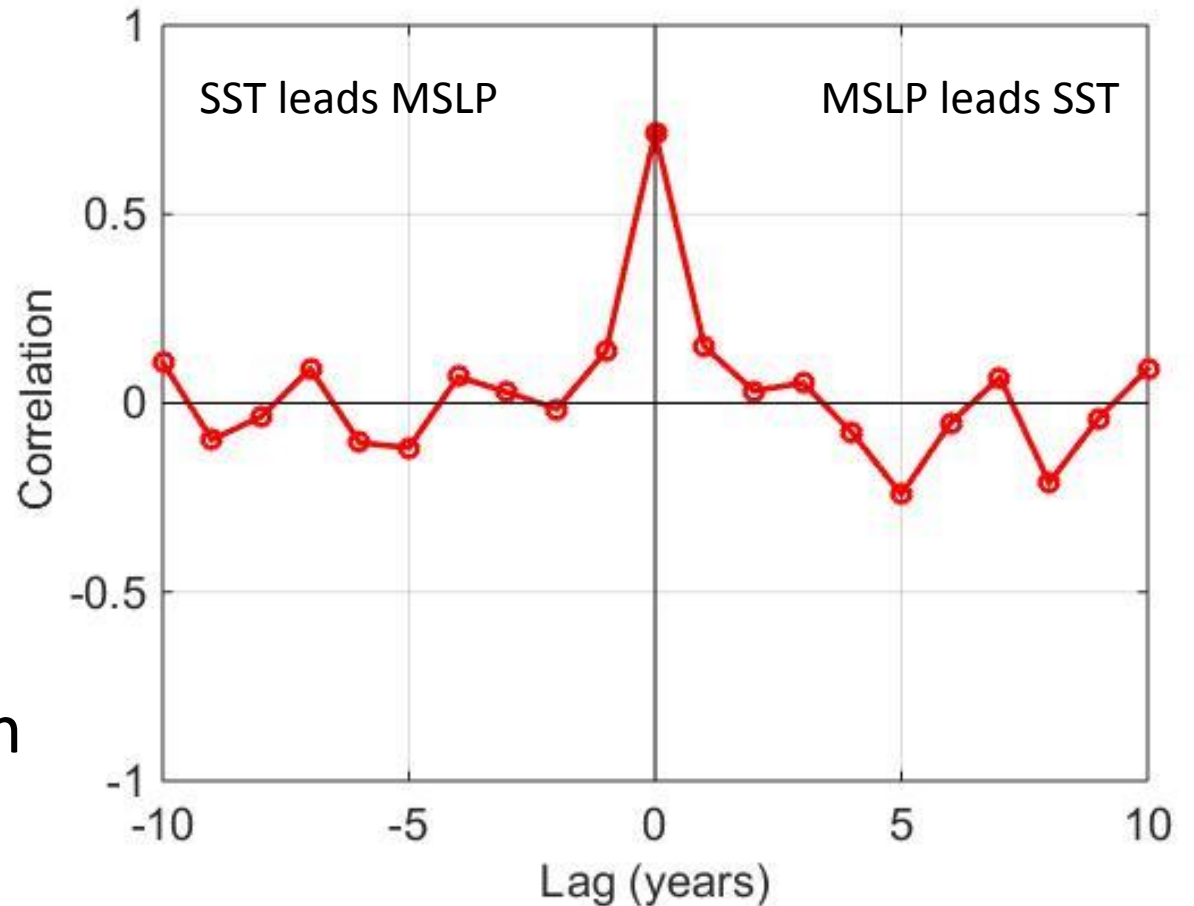
- Monthly statistics:

SST 1-month autocor = 0.92

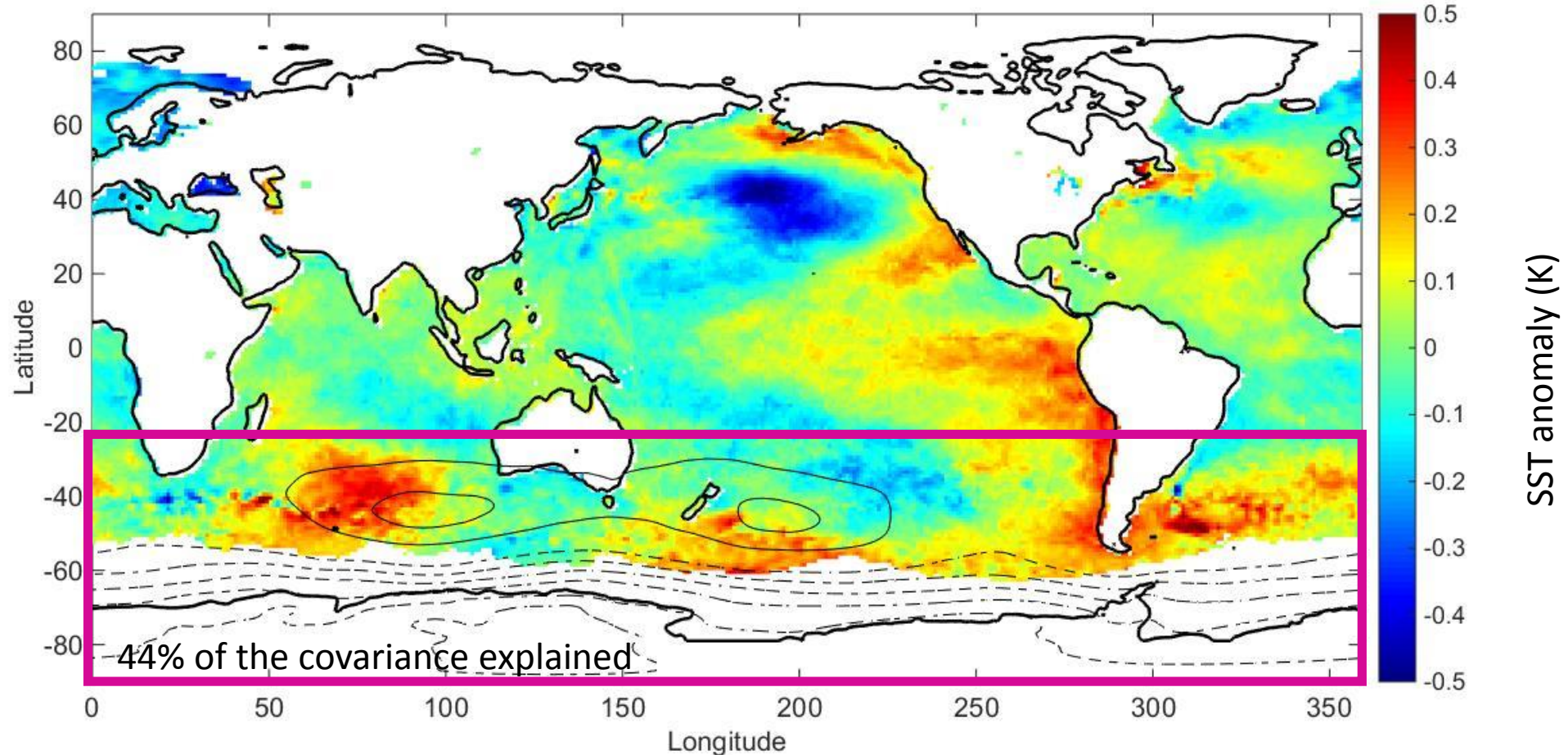
MSLP 1-month autocor = 0.41

Cross-corr: 0.44, 0.54, 0.64

- Longer timescale statistics: strong covariability; no stat. significant delay but decadal oscillation seen in each field separately (not shown)  
→ “stationary oscillation”



# SST (color) / MSLP (ci=1hPa) Southern Ocean (Max Cov. Ana., ERA20C, J-J-A 1960-2010)



**NB** Analysis extended globally via linear regression

# SST / MSLP statistics for the Southern Ocean (Max Cov. Ana., ERA20C, J-J-A 1960-2010)

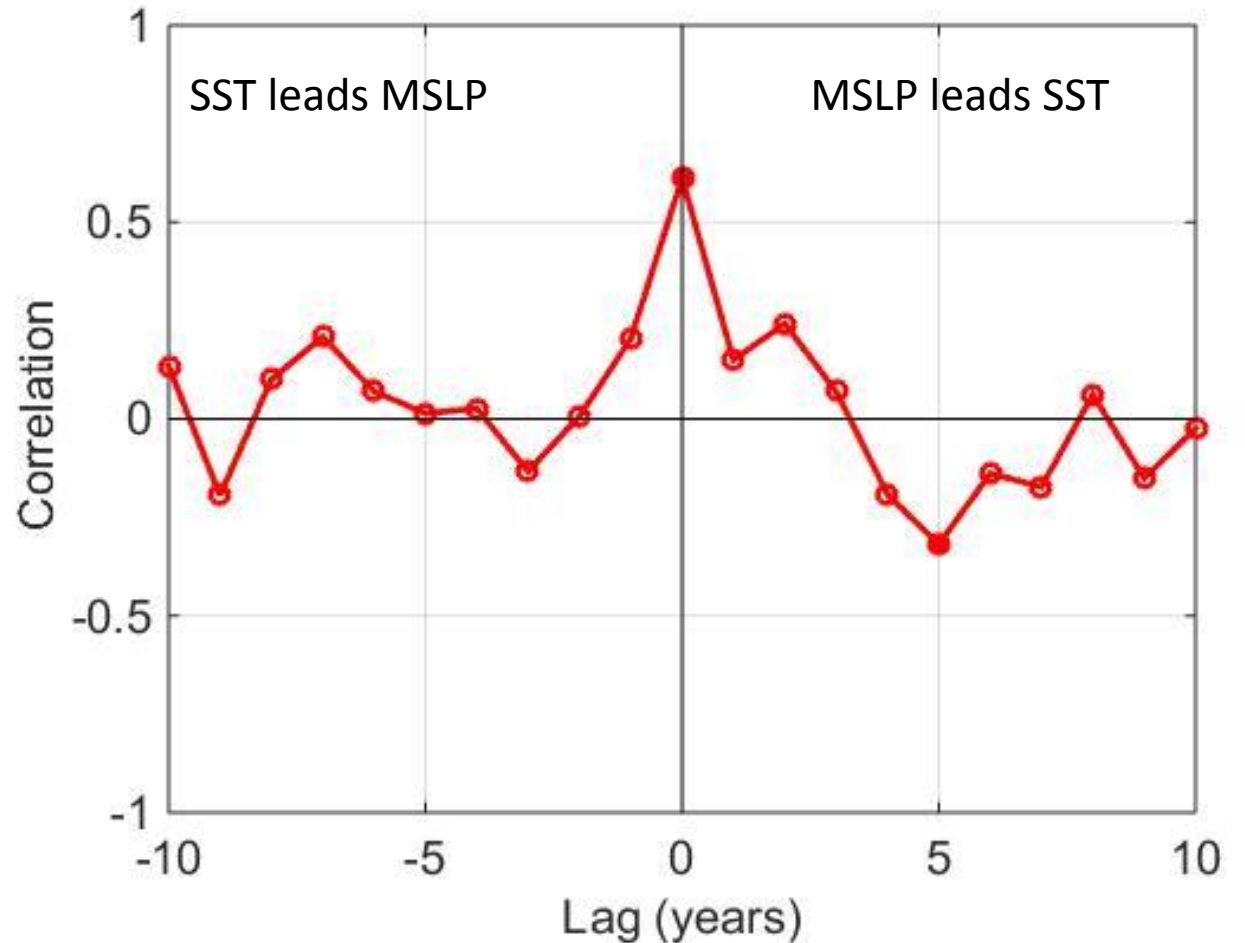
- Monthly statistics:

SST 1-month autocor = 0.89

MSLP 1-month autocor = 0.18

Cross-corr: 0.34, 0.43, 0.45

- Longer timescale statistics:  
indication of decadal oscillation,  
with a reversal of SST pattern 5  
years after MSL

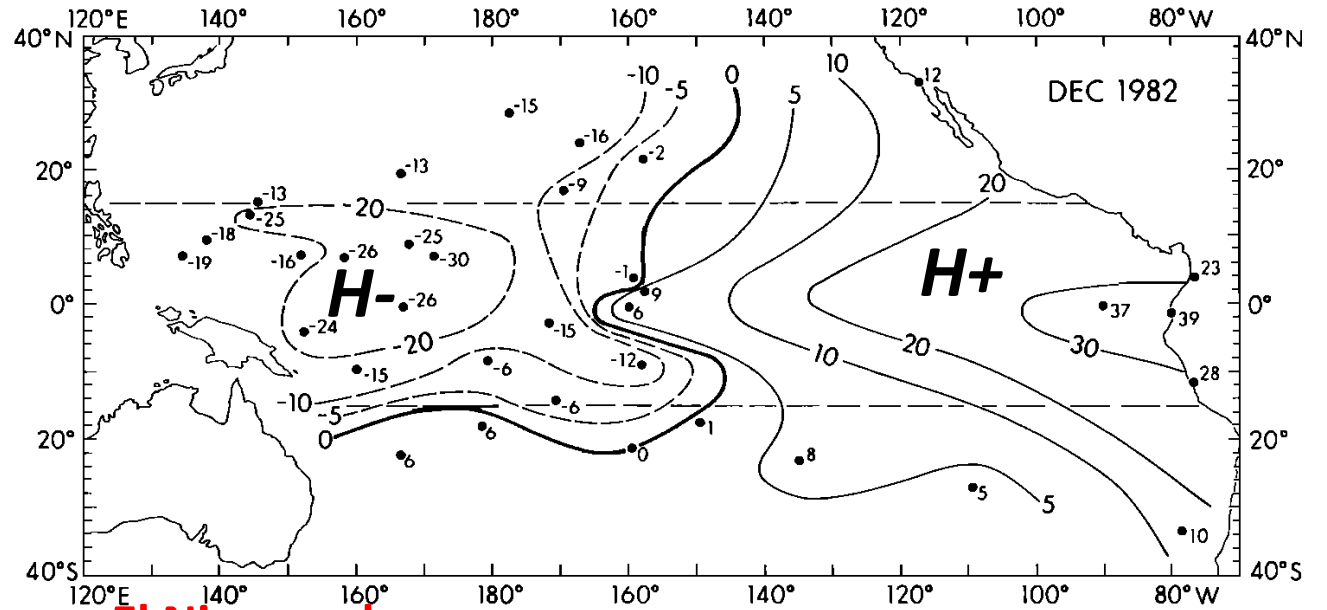




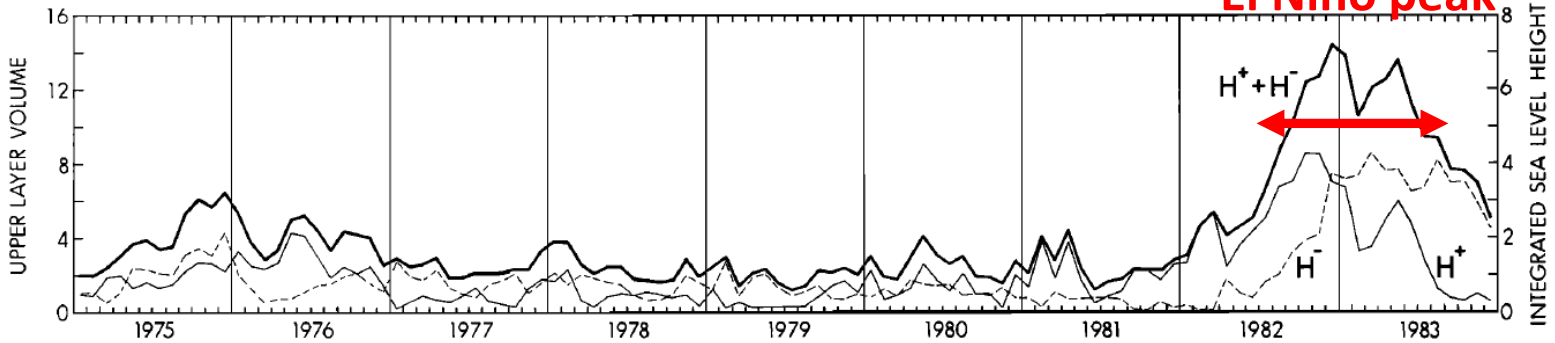
# Wyrtki's (1985) view of El Nino

- El Nino = burst event to release heat stored in the equatorial Pacific

Sea level anomalies in December 1982 (cm)



El Nino peak

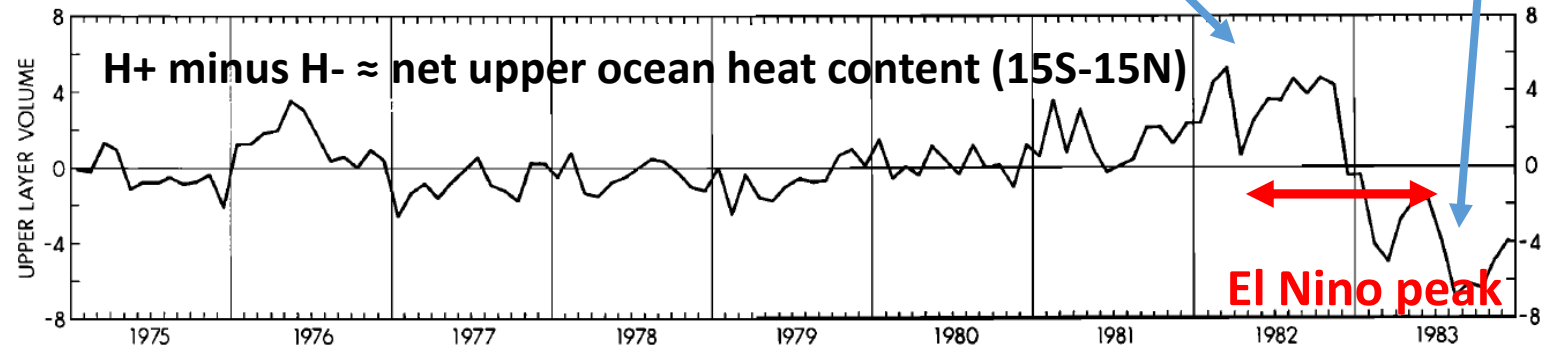


Heat builds up in the Tropical Pacific

Heat is exported away from the Tropical Pacific

NB: mean volume is ~70 in this unit

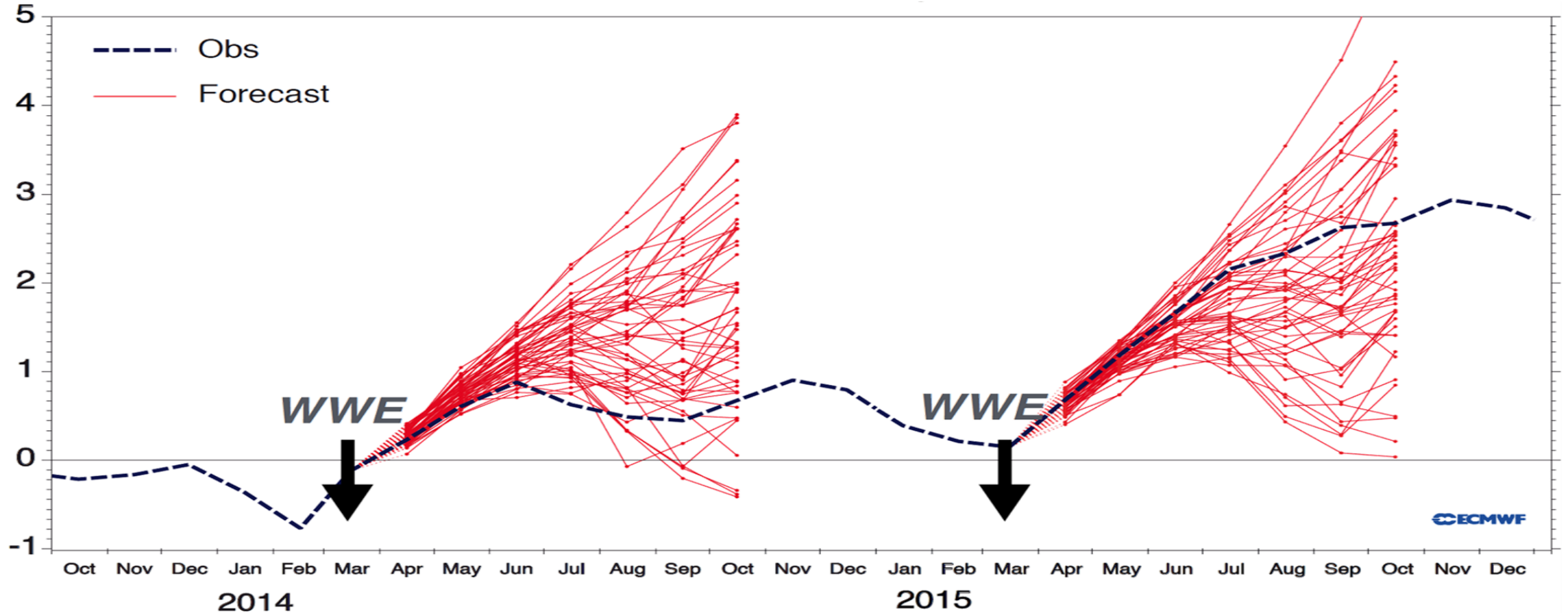
NB2: See Mayer et al. (2016) for the full energy budget view



# Wyrkti's (1985) view of El Nino

- “The explanation of an El Nino cycle as a combination of atmospheric randomness and a deterministic ocean might be unpleasing to many scientists, but it probably characterizes correctly the interaction between the two media”

# Predictive skill in the Tropics: “La Nada 2014”

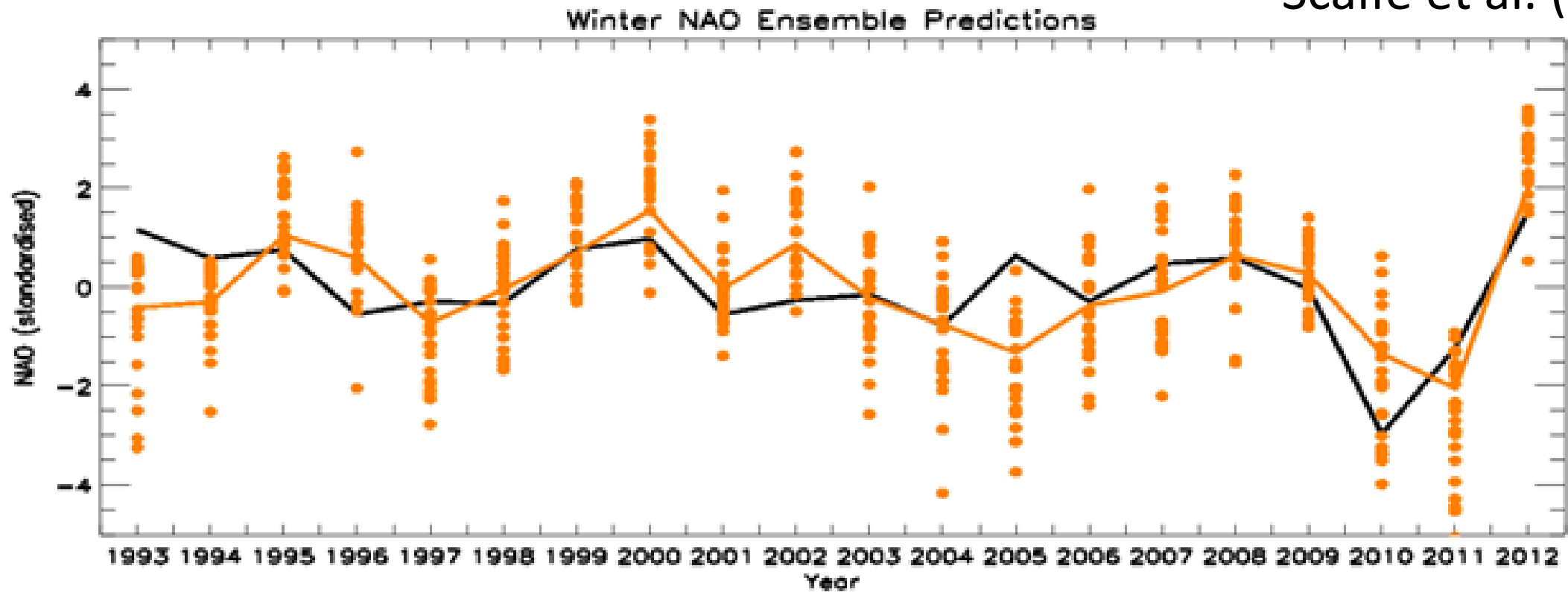


(slide courtesy of J. Vialard)

See also McPhaden (2015)

# Predictive skills in the extra-tropics

Scaife et al. (2014)

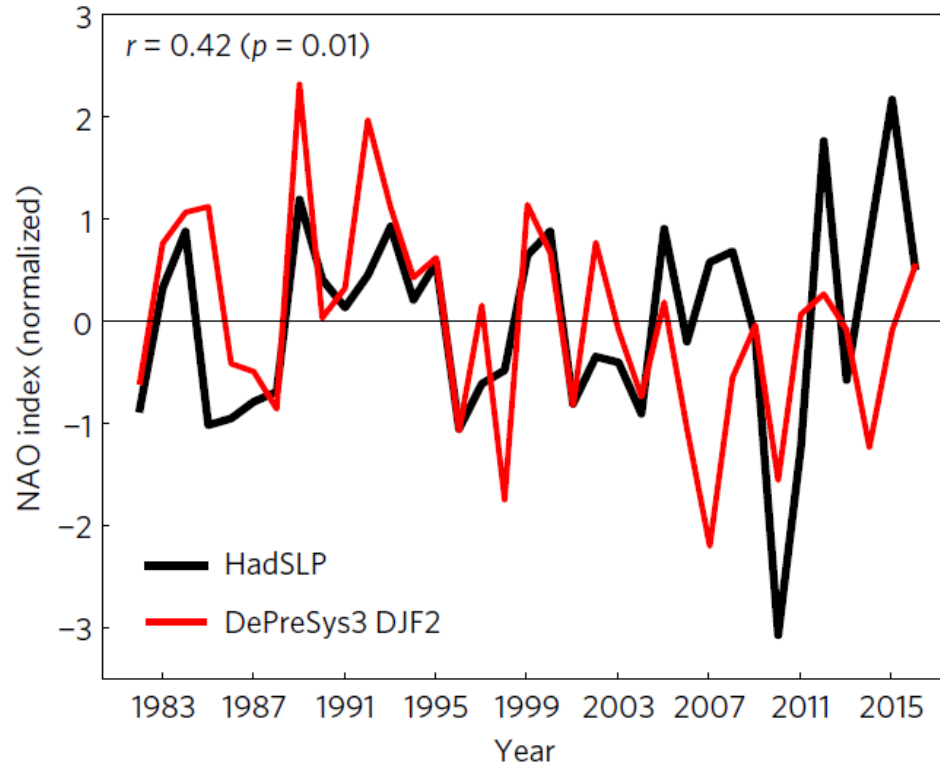


DJF NAO predicted from coupled predictions (GLOsea5) initialised on Nov 1st

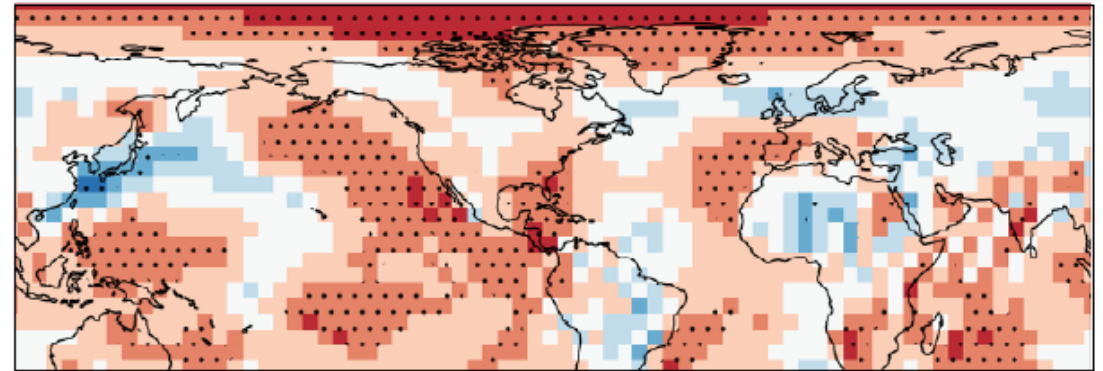
# Predictive skills in the extra-tropics

Dunstone et al. (2016)

## NAO index

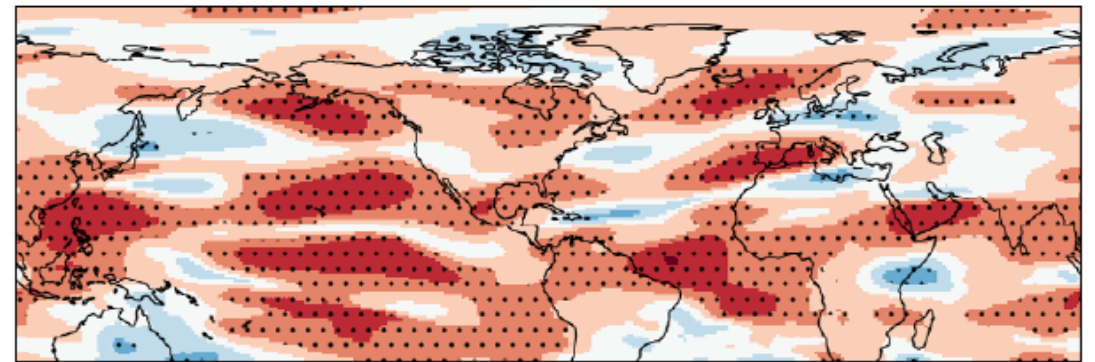


MSLP second-winter skill



f

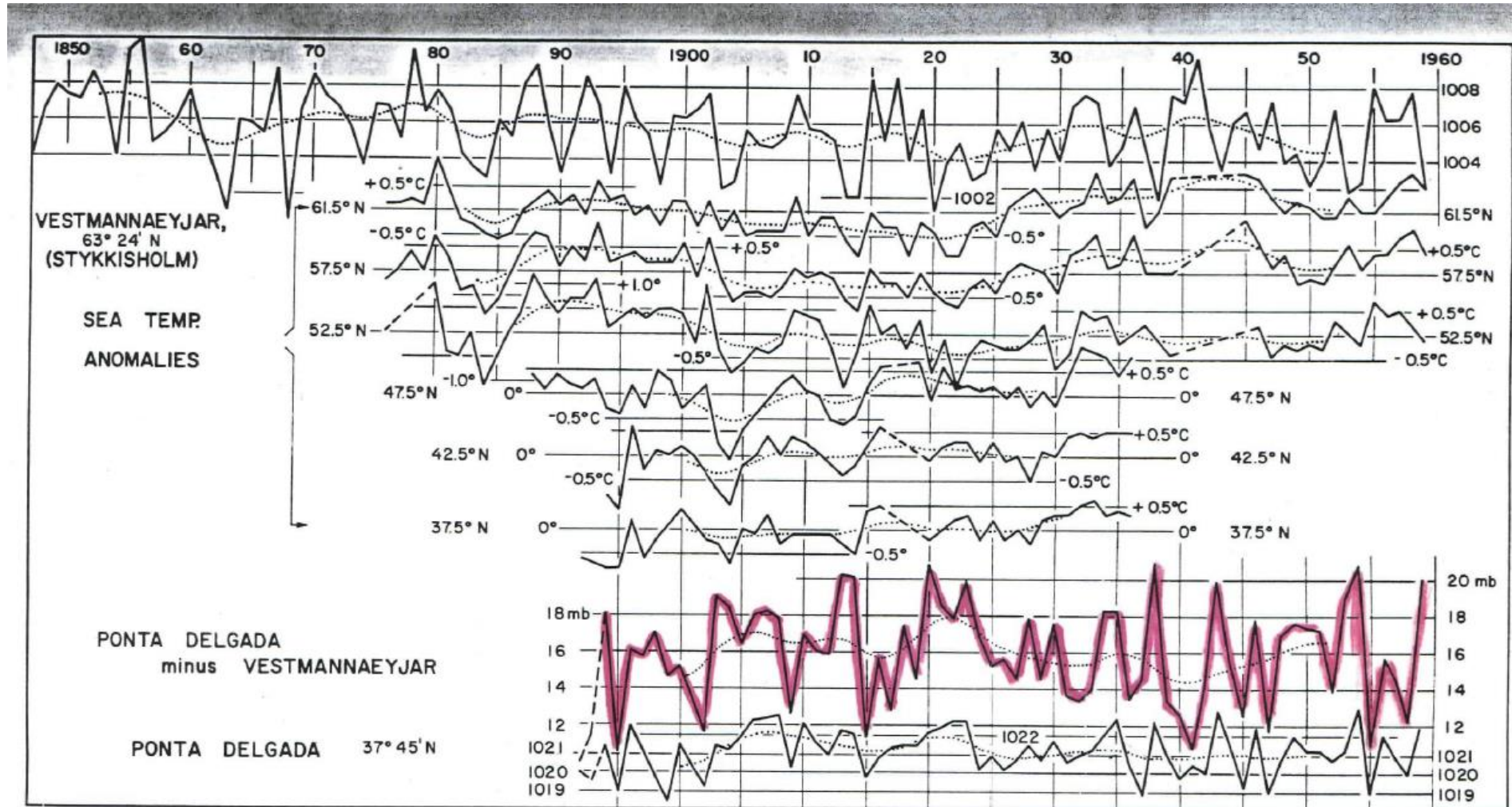
U250 second-winter skill



“2<sup>nd</sup>” DJF NAO predicted from coupled predictions initialised on Nov 1st



# Bjerknes (1964): Atlantic air-sea interactions



# The role of ocean advection in altering SST

- The high latitude (>50N) correlation between strength of the westerlies and SST remains <0 for “short” and “long trends” (19-yr smoothing used)
- This contrasts with the 40-50N belt where positive correlations appear on long timescales

TABLE III. Correlation of short-period residuals of sea temperature versus pressure difference Ponta Delgada minus Vestmannaeyar.

“Short trend”

Period	Test field	Corr. coeff.
1900–1928	61.5°N	−0.48
1900–1928	57.5°N	−0.64
1900–1928	52.5°N	−0.72
1900–1928	47.5°N	−0.65
1900–1928	42.5°N	−0.45
1900–1928	37.5°N	−0.45

TABLE II. Correlation of sea temperature versus pressure difference Ponta Delgada minus Vestmannaeyar, all data identically smoothed.

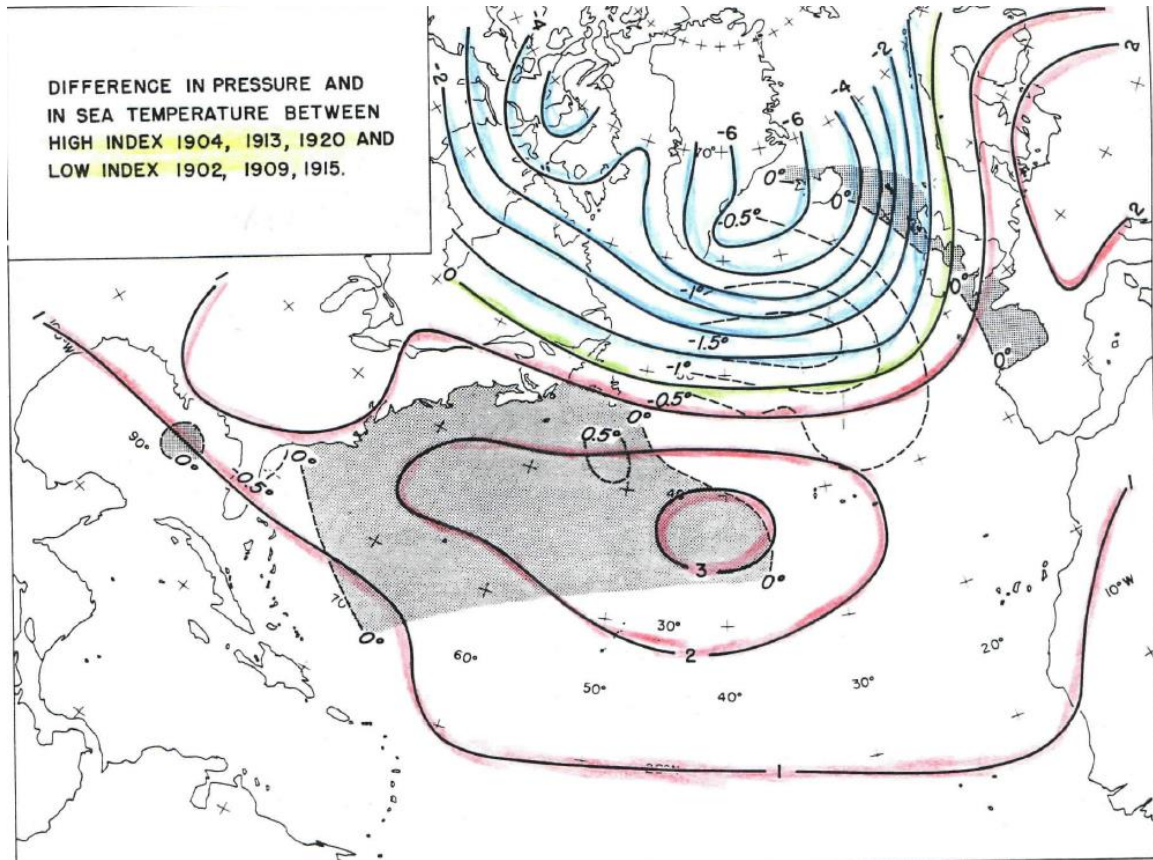
“Long trend”

Period	Test field	Corr. coeff.
1900–1928	61.5°N	−0.34
1900–1928	57.5°N	−0.82
1900–1928	52.5°N	−0.82
1900–1928	47.5°N	0.18
1900–1928	42.5°N	0.33
1900–1928	37.5°N	−0.37

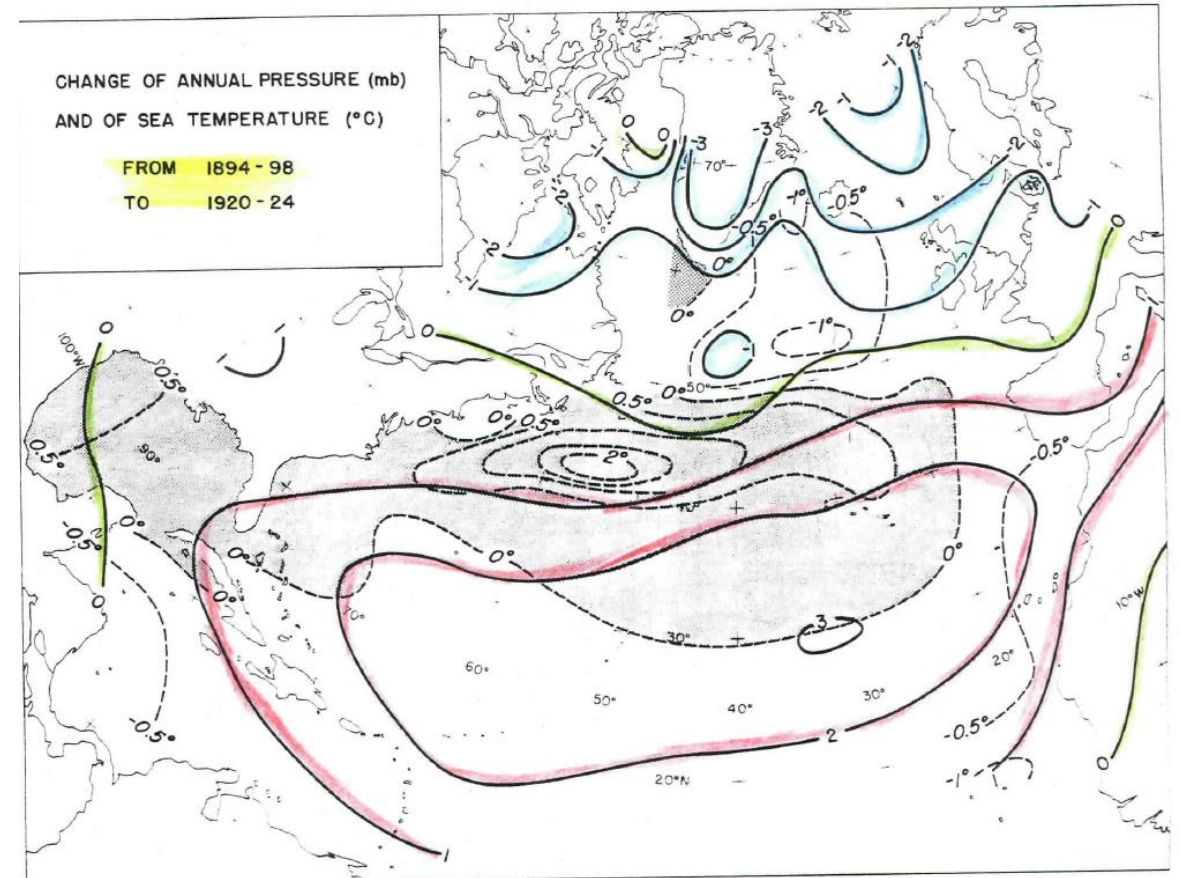
olve

# Spatial patterns of MSLP and SST

***“Short trends of change”***



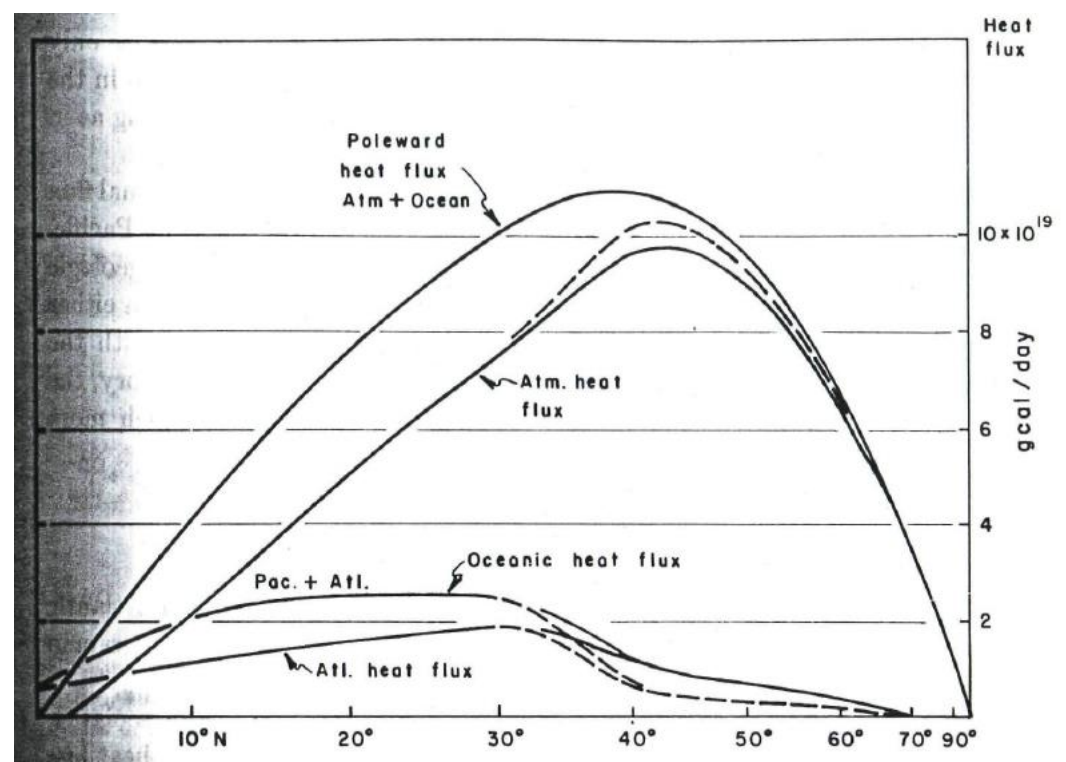
***“Long trends of change”***



**NB** The pre / post 1950 records do not agree on spatial pattern (Deser and Blackmon, 1993)

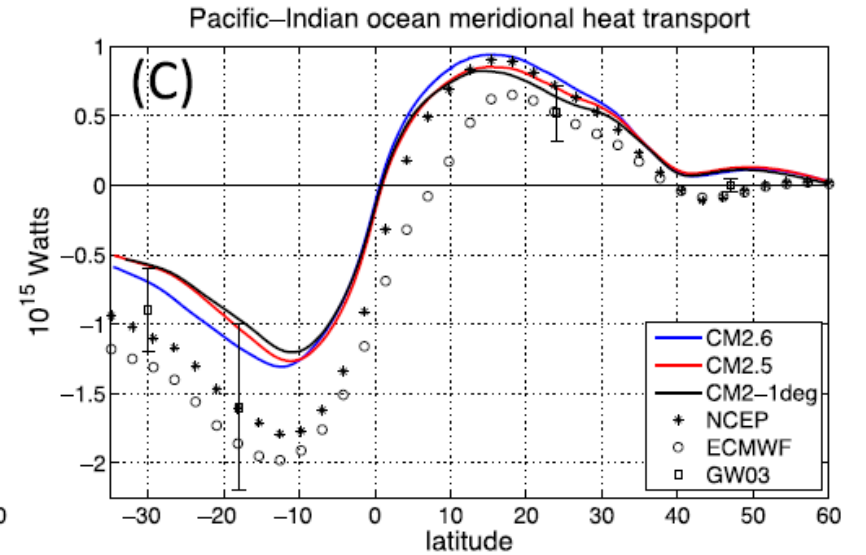
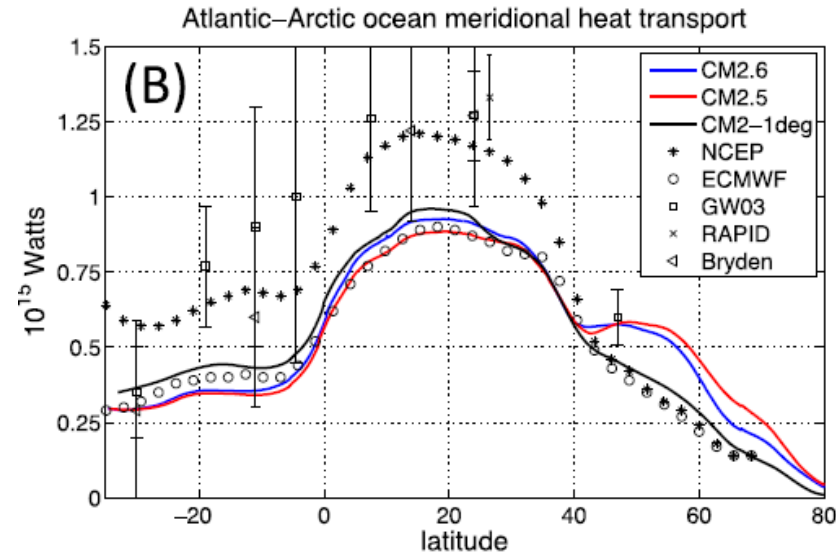


# Bjerknes' compensation hypothesis



- Mechanistically, periods of weak westerlies have higher than normal  $H_a$ , but also lead to a weakening of the Gulf Stream and a weaker  $H_o$ , thus re-establishing a constant total ( $H_o + H_a$ ) poleward heat transport
- Climate variability reflects compensating fluctuations in oceanic ( $H_o$ ) and atmospheric ( $H_a$ ) poleward heat transports, without significant changes in the top-of-the-atmosphere radiative budget

# Bjerknes' compensation hypothesis



Griffies et al. (2015)

- Because the Atlantic is the main contributor to oceanic poleward heat transport (>40N), it plays a leading role in “natural” climate fluctuations.
- Bjerknes' monograph is unclear as to causality and can be read as reflecting a passive response of the ocean to the atmosphere. But it has opened the way to much emphasis on driving of climate variability by the midlatitude oceans.

## 2. How do SST changes affect the atmosphere above the boundary layer?

- Diabatic heating processes
- Theory: prescribe a heat source and predict the atmospheric circulation response
- Challenge: apply the theory to observations and realistic numerical experiments

# Diabatic heating processes

- Any process adding or removing heat to/from air parcels:
- Exchange with Space: radiation (absorption or shortwave, absorption/emission of longwave radiation)
- Exchange with the lower boundary (ocean, land, ice): radiative and turbulent heat fluxes (“sensible” heat flux)
- Phase change: depending whether one works with dry or moist potential temperature, this is taken as an exchange with the lower boundary (surface evaporation) or an internal heat source (latent heat release) –see Emmanuel, 2000; Pauluis et al., 2010.

# Diabatic heating in models (GCMs or diagnostics)

$$\frac{\partial \theta}{\partial t} + \mathbf{v} \cdot \nabla \theta = Q_{diab}$$

- Need distinguishing between resolved ( $\langle \rangle$ ) and unresolved ( $\ast$ ) processes, or slow ( $\langle \rangle$ ) and fast ( $\ast$ ) motions:

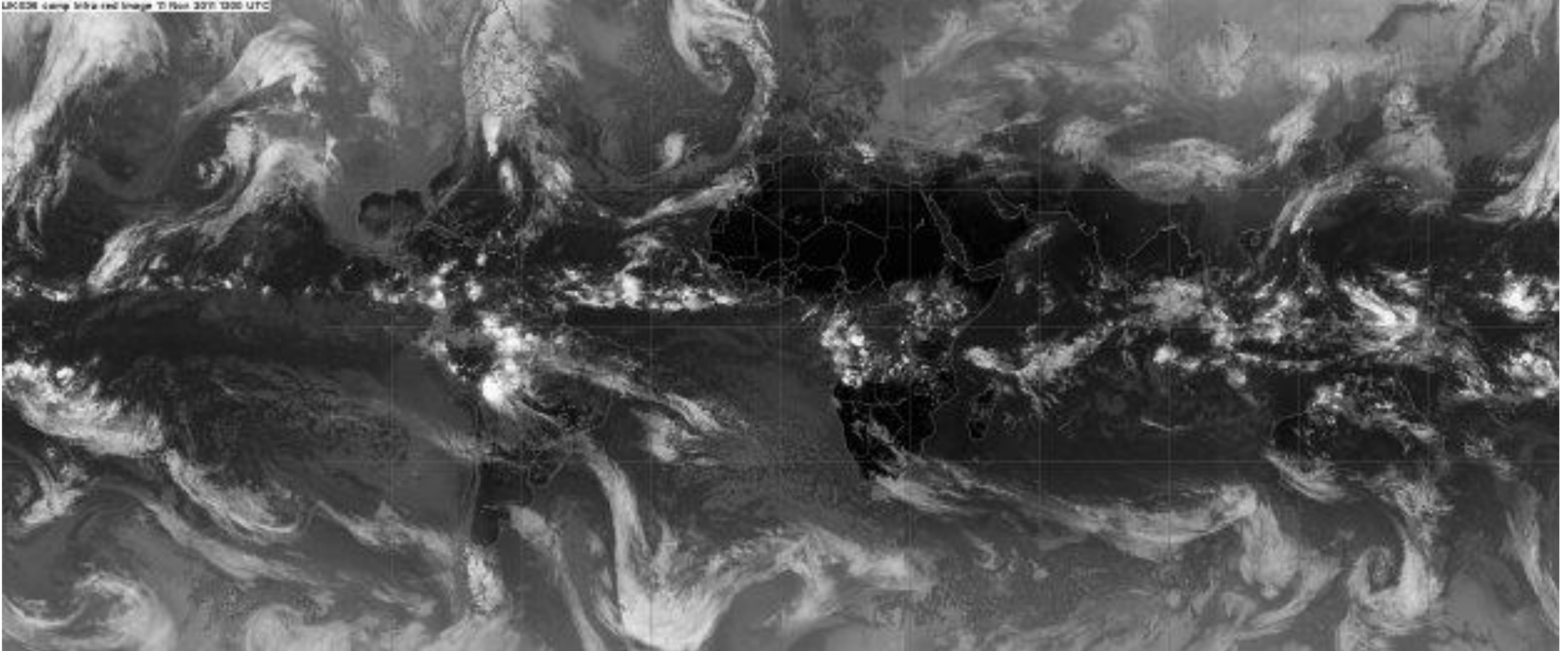
$$\frac{\partial \langle \theta \rangle}{\partial t} + \langle \mathbf{v} \rangle \cdot \nabla \langle \theta \rangle = \langle Q_{diab} \rangle - \nabla \cdot \langle \mathbf{v}^* \theta^* \rangle \quad (1)$$

with  $\langle Q_{diab} \rangle = \langle Q_{rad} \rangle + \langle Q_{phase} \rangle + \langle Q_{sen} \rangle$

- The terms on the r.h.s of (1) represent an *apparent heating* for the resolved flow which can be quite different from the assumed diabatic heating taking place:

$$\langle Q_{app} \rangle = \langle Q_{diab} \rangle - \nabla \cdot \langle \mathbf{v}^* \theta^* \rangle$$

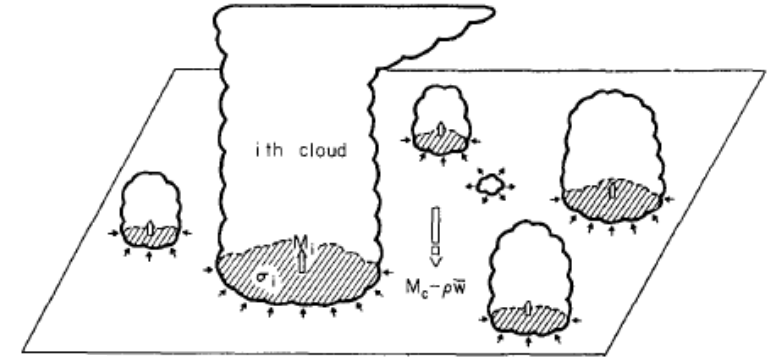
# Diabatic heating: two examples



*Global Infrared image (snapshot): white = cold = cloud tops*

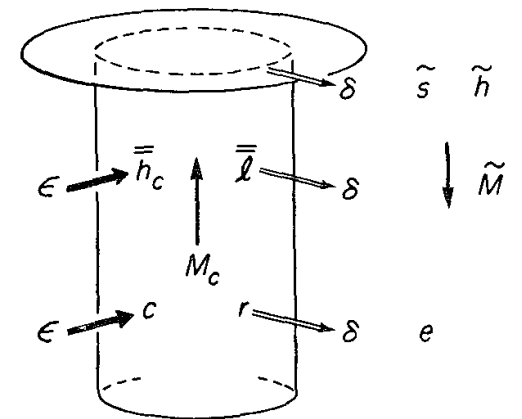
# Diabatic heating example 1: cumulus parameterisation (e.g., Yanai et al. 1973)

- Neglecting horizontal effects:



$$\langle Q_{app} \rangle = \langle Q_{diab} \rangle - \nabla \cdot \langle \mathbf{v}^* \theta^* \rangle \approx \langle Q_{diab} \rangle - \frac{\langle w^* \theta^* \rangle}{\partial z}$$

- ...and using an idealised entrainment/detrainment model for the cloud ensemble, one can obtain an expression for the apparent heating:

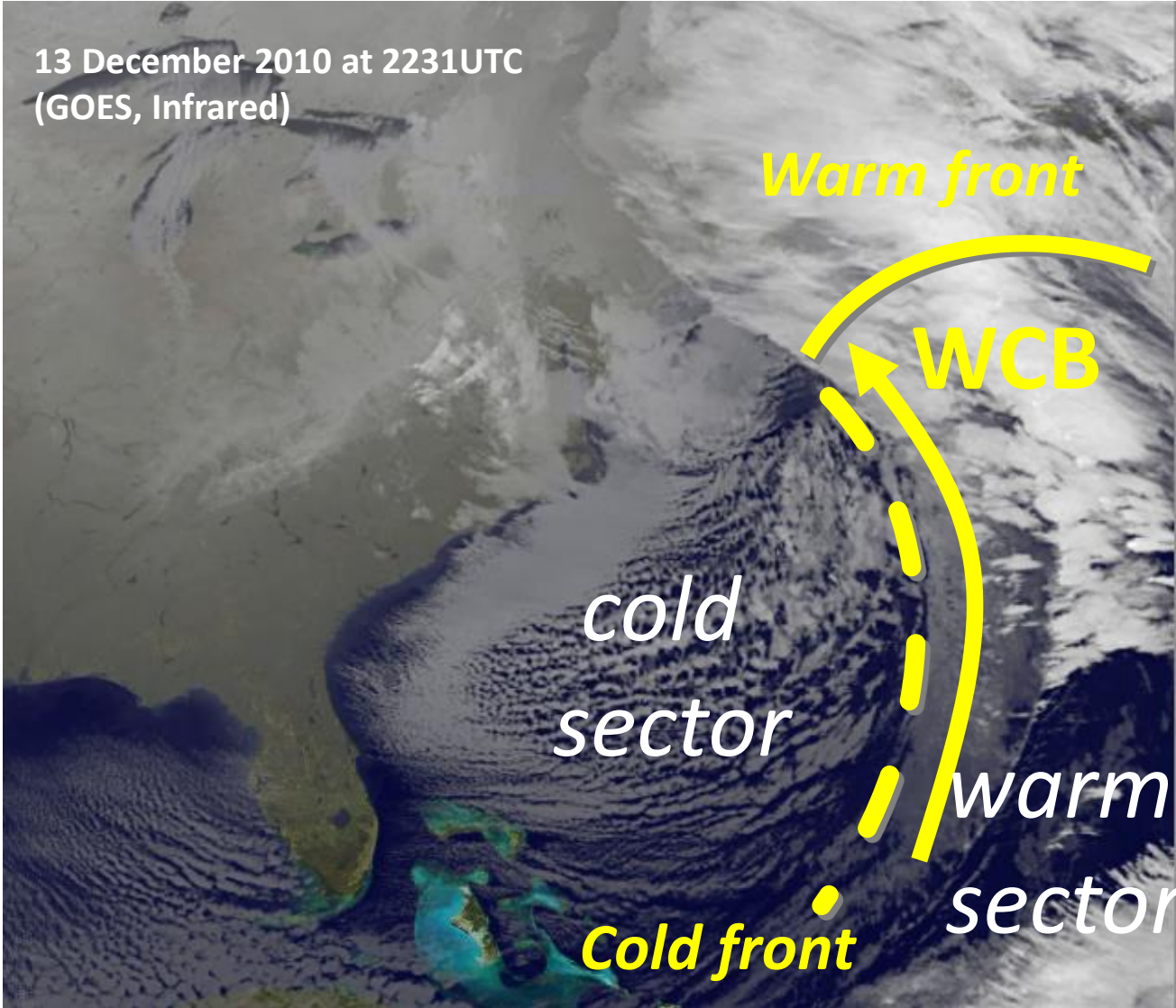


$$\langle Q_{app} \rangle \approx \langle Q_{rad} \rangle + \langle Q_{sen} \rangle + M_c \frac{\partial \langle \theta \rangle}{\partial z} - l_v e$$

Warming due to compensating subsidence (M<sub>c</sub>=cloud mass flux)

Cooling due to re-evaporation of cloud droplets

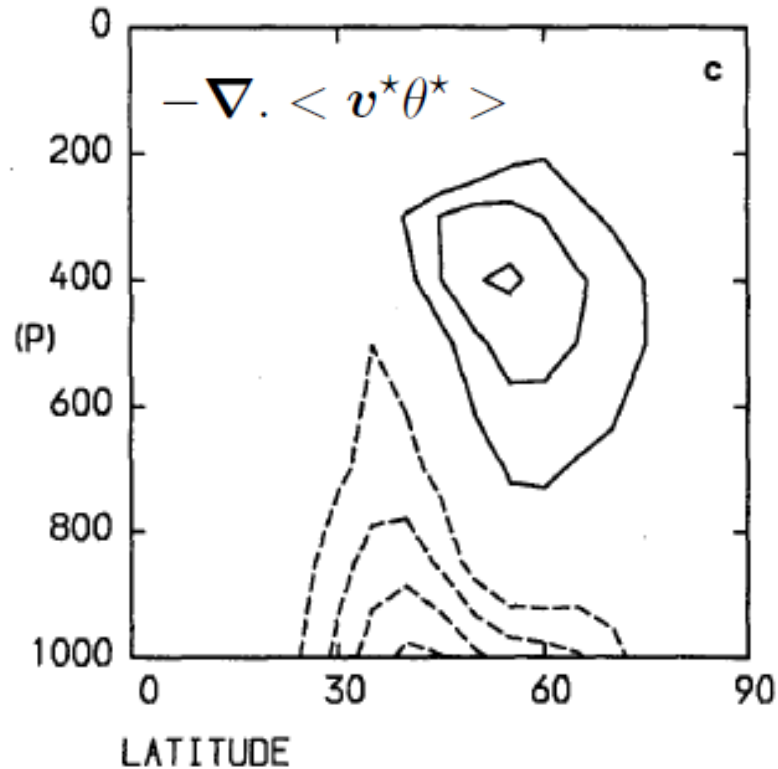
# Diabatic heating example 2: Extra-tropical cyclones



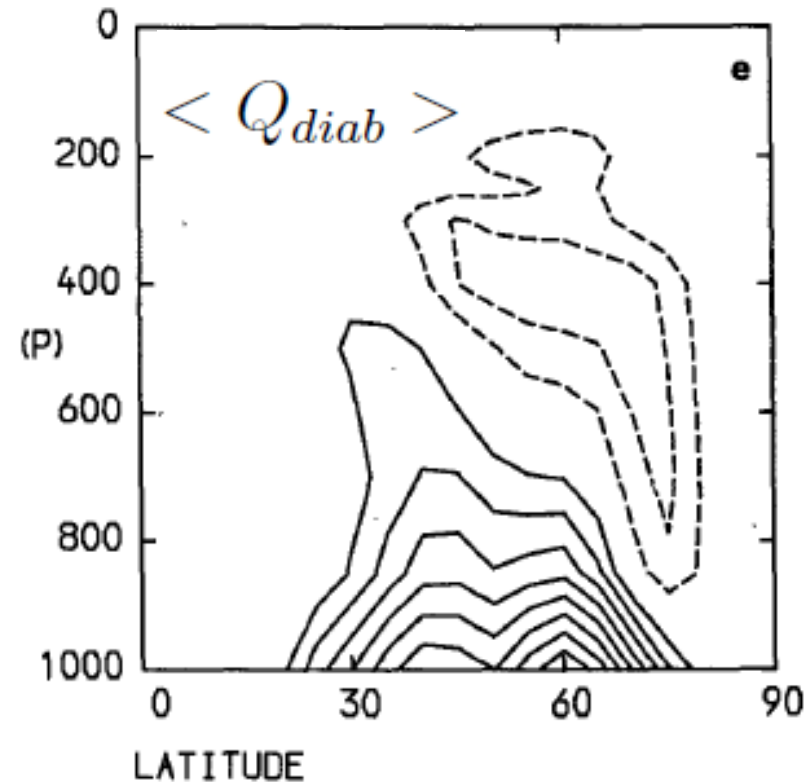


# Diabatic heating example 2: extra-tropical cyclones or “storm-track” (Hoskins & Valdes, 1990)

Averaged heating over the Northwest Atlantic (CI=0.25K/day)



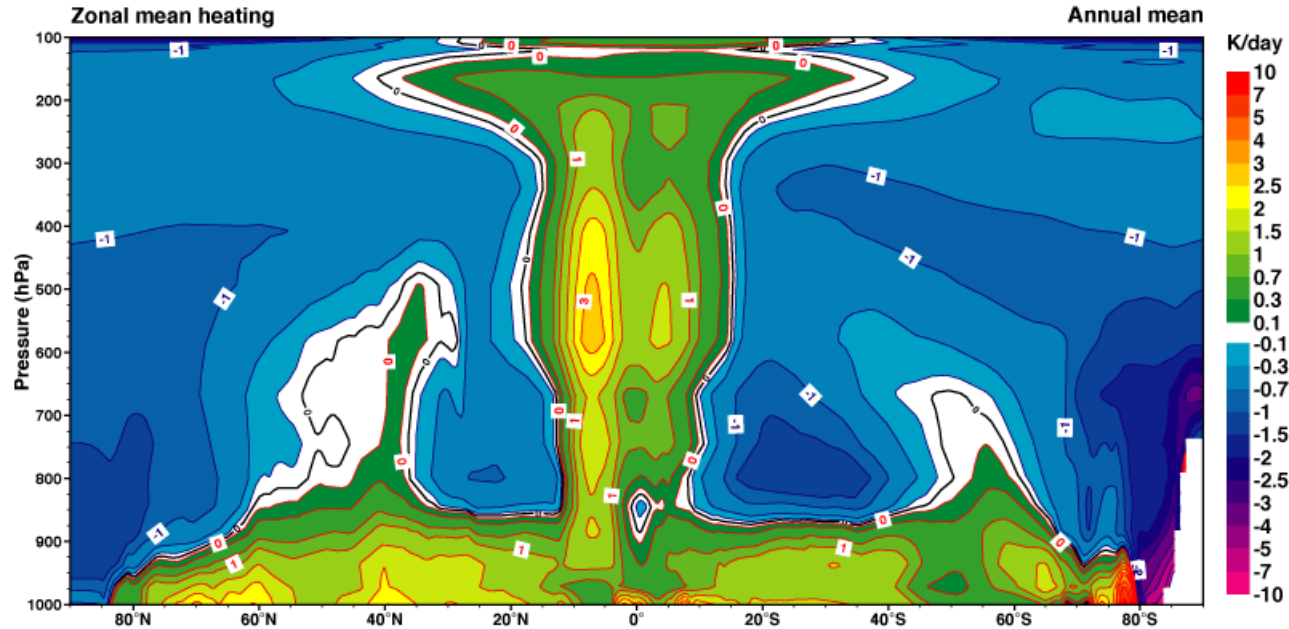
NB 2.5-6 day high-pass filter applied



- $Q_{app}$  is a small residual between diabatic heating and thermal forcing by eddies

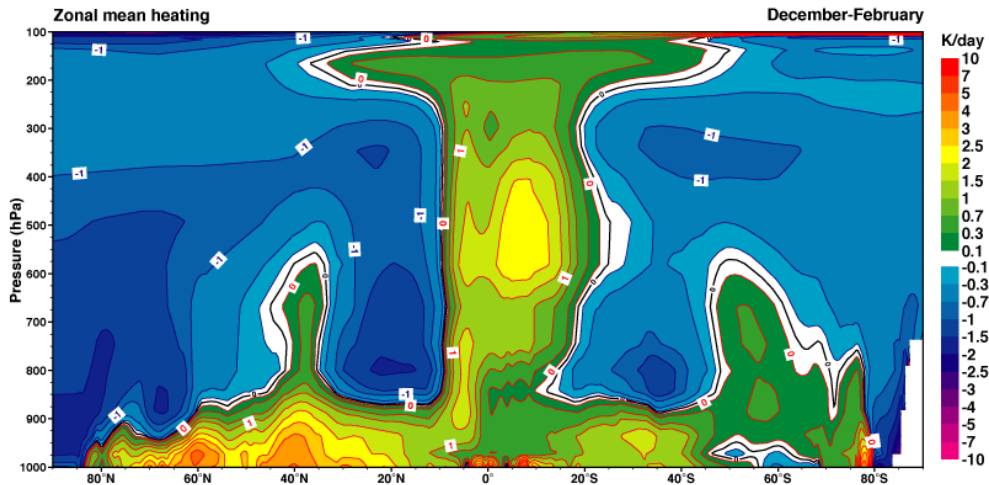
# Qdiab climatology from ERA40 atlas (K/day)

Annual  
mean

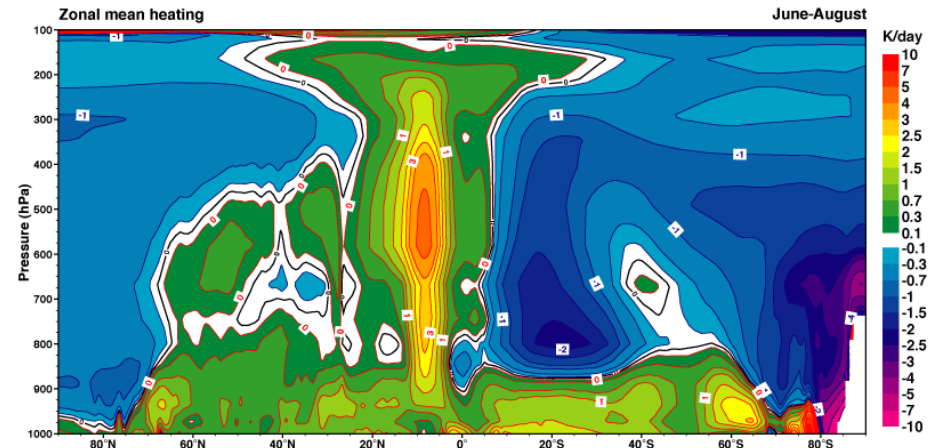


**NB** Computed from the net forecast tendency as a residual in the thermodynamic equation

DJF



JJA



# Response of the atmosphere (temp., winds) to a prescribed heating anomaly

- Goal is to gain understanding as to what maintains a climatic anomaly or perturbation (e.g., a positive phase of the NAO or El Nino conditions averaged over many such events)
- The overbar represent the “normal” state while primes denote the “anomalous” state
- Need to do this to increase our confidence that numerical models do the right thing

# Basic theory: Hoskins and Karoly (1981)

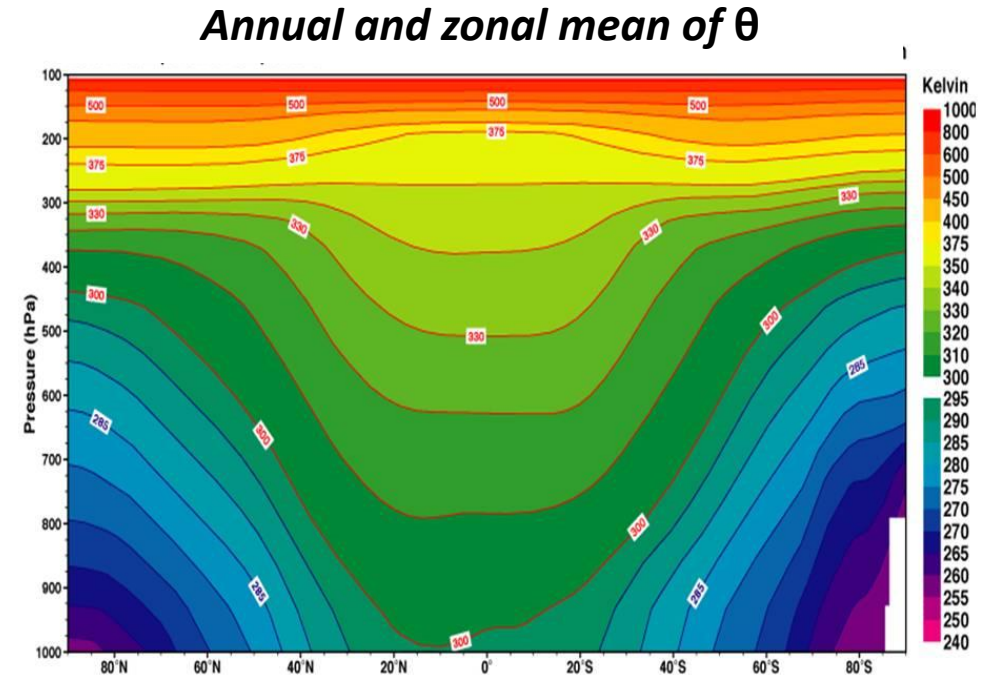
*NB Notes provide derivation of this model*

- Basic state (overbar) = zonal flow in thermal wind balance
- Forcing: prescribed heat source
- Frictional effects entirely neglected
- Perturbations (primes) are geostrophic and obey linear conservation of vorticity and heat (entropy):

$$\bar{u} \xi_x' + \beta v' = f w_z',$$

$$\bar{u} \theta_x' + v' \bar{\theta}_y + w' \bar{\theta}_z = (\theta_0/g) Q.$$

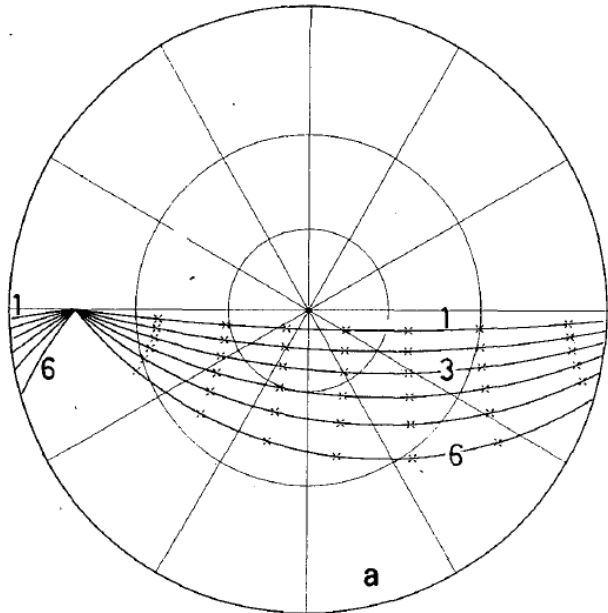
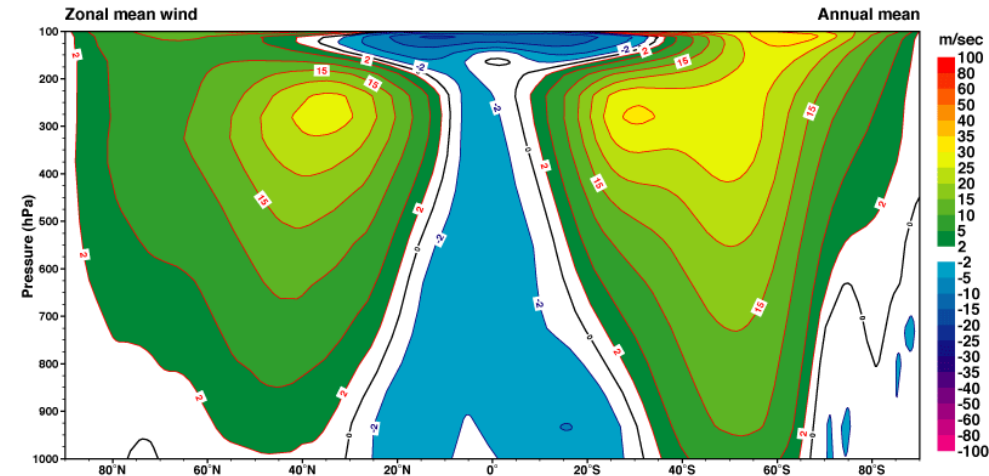
Prescribed  
heat source



# Basic theory: Hoskins and Karoly (1981)

- Because the zonal winds increase with height in the troposphere, the zonal advection term is more important at upper than at lower levels.
- At upper levels, vorticity conservation is a stationary Rossby wave equation:

*Annual and zonal mean of U*

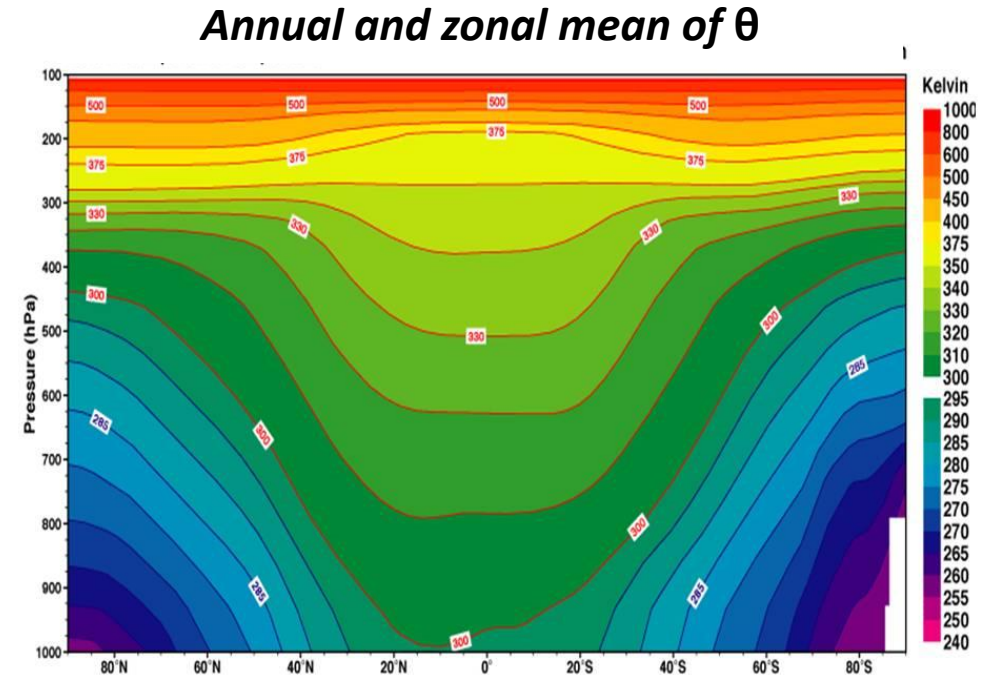


$$\bar{u} \xi_x' + \beta v' = f w_z'$$

Localized Rossby wave source → remote forcing of wind anomalies (anticyclones generated above ascending regions)

# Basic theory: Hoskins and Karoly (1981)

- Simplification: we restrict ourselves to lower levels and long waves ( $>1000$  km) for which vorticity conservation reduces to Sverdrup balance:



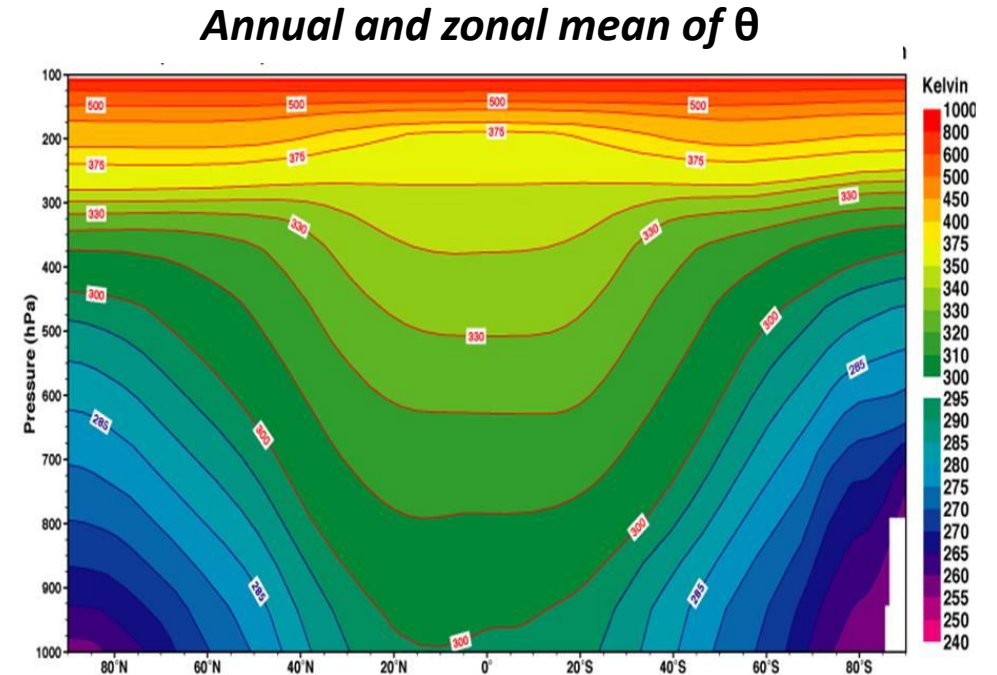
$$\cancel{\bar{u} \bar{\theta}_x'} + \beta v' = f w_z'$$

$$\bar{u} \theta_x' + v' \bar{\theta}_y + w' \bar{\theta}_z = (\theta_0/g) Q.$$

Remember  
David's lecture  
yesterday

# Basic theory: Hoskins and Karoly (1981)

- Qualitative understanding by looking under which conditions we can simply consider only one term on the l.h.s of the heat equation:

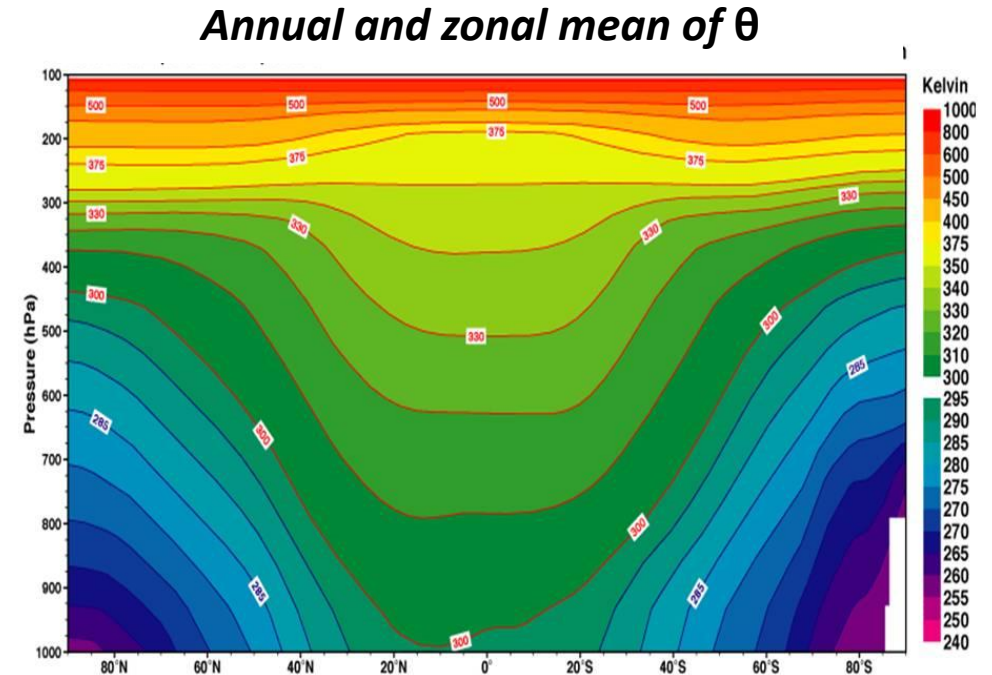


~~$$\bar{u} \theta_x'$$~~ + 
$$\beta v' = f w_z'$$

$$\bar{u} \theta_x' + v' \bar{\theta}_y + w' \bar{\theta}_z = (\theta_0/g) Q. \quad ?$$

# Basic theory: Hoskins and Karoly (1981)

- Qualitative understanding by looking under which conditions we can simply consider only one term on the l.h.s of the heat equation:



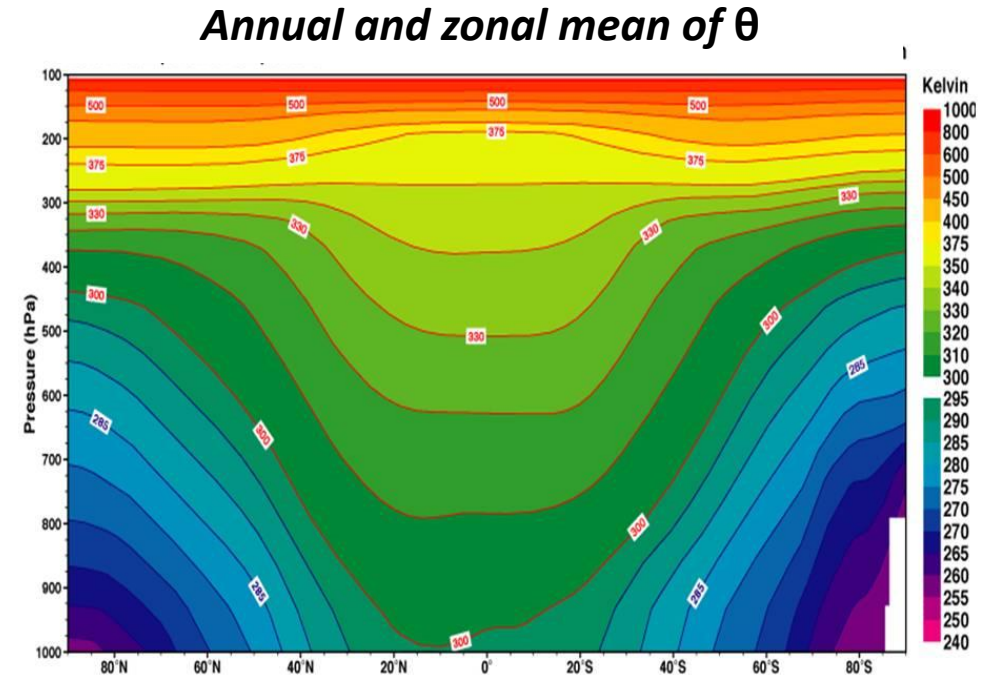
$$\cancel{\bar{u} \theta_x'} + \beta v' = f w_z'$$

$$\bar{u} \theta_x' + v' \bar{\theta}_y + w' \bar{\theta}_z = (\theta_0/g) Q. \quad ?$$



# Basic theory: Hoskins and Karoly (1981)

- Qualitative understanding by looking under which conditions we can simply consider only one term on the l.h.s of the heat equation:



~~$$\bar{u} \theta_x'$$~~ + 
$$\beta v' = f w_z'$$

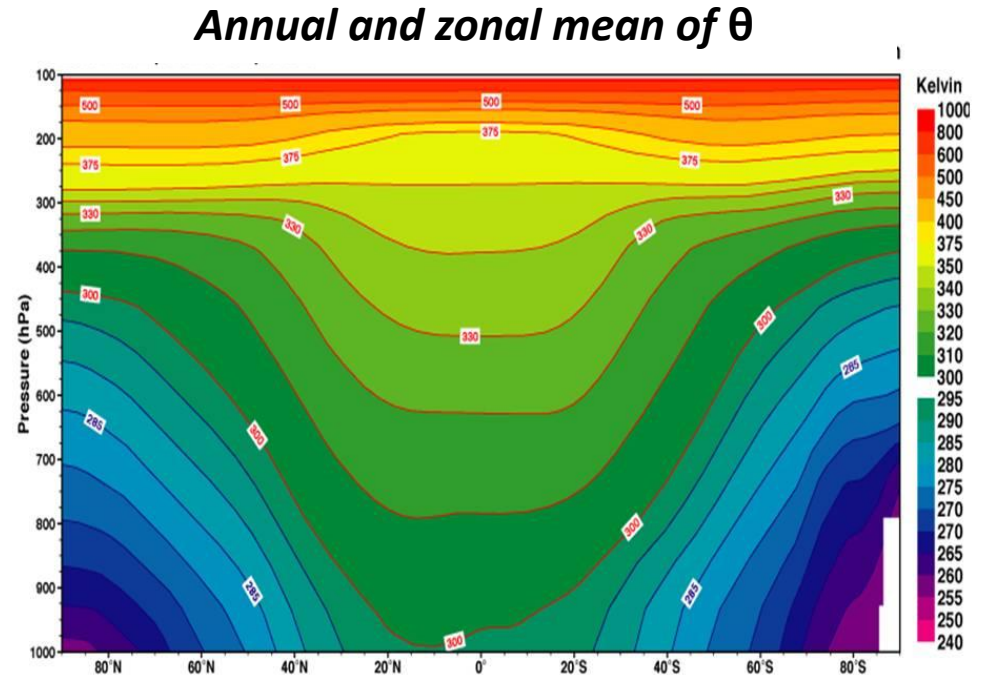
$$\bar{u} \theta_x' + v' \bar{\theta}_y + w' \bar{\theta}_z = (\theta_0/g) Q. \quad ?$$

# Basic theory: Hoskins and Karoly (1981)

- Use the thermal wind to rewrite the heat equation as:

Buoyancy frequency

$$N^2 = \frac{g}{\theta_0} \frac{d\theta}{dz}$$



$$f\bar{u}v'_z - f\bar{u}_z v' + w'N^2 = Q.$$

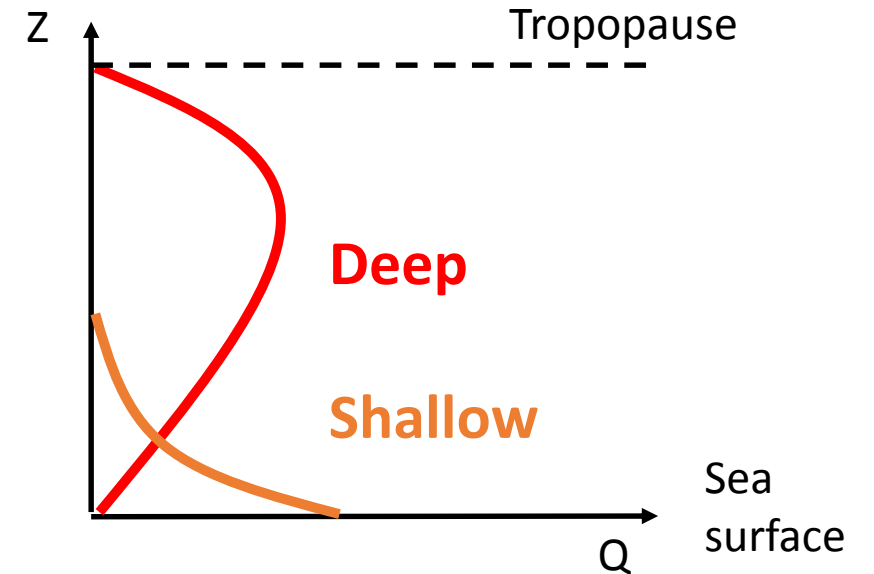
Zonal advection of heat
Meridional advection of heat
Vertical advection of heat

# Basic theory: Hoskins and Karoly (1981)

- If zonal advection of heat dominates, then:

$$v' \simeq Q H_Q / f \bar{u} \quad \text{with} \quad H_Q \equiv Q / Q_z$$

(a few kms for shallow source, 5-10km for a deep source)



$$f \bar{u} v_z'$$

Zonal advection  
of heat

$$- f \bar{u}_z v'$$

Meridional  
advection of heat

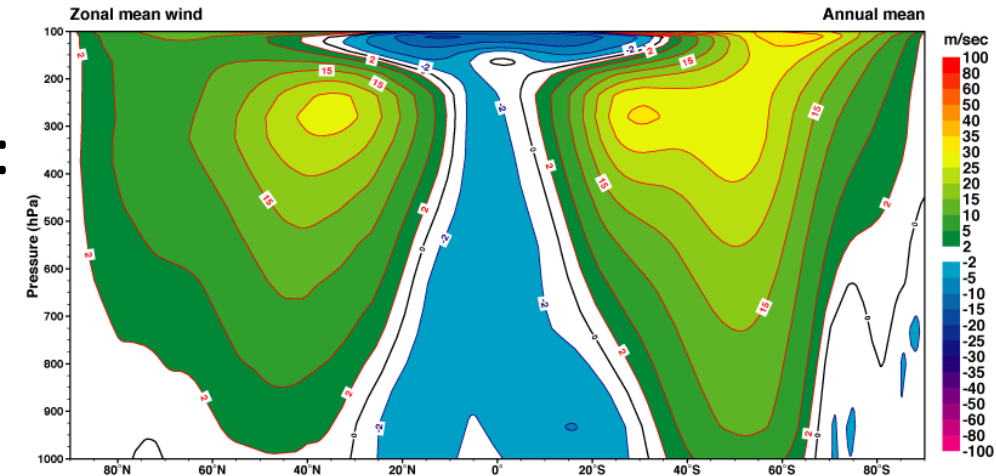
$$+ w' N^2$$

Vertical advection  
of heat

$$= Q.$$

# Basic theory: Hoskins and Karoly (1981)

*Annual and zonal mean of U*



- If meridional advection of heat dominates, then:

$$v' \simeq Q / f \bar{u}_z = Q H_u / f \bar{u} \quad \text{with} \quad H_u \equiv \bar{u} / \bar{u}_z$$

$$\sim 10 \text{ms}^{-1} / (30 \text{ms}^{-1} / 10 \text{km}) \sim 3 \text{km}$$

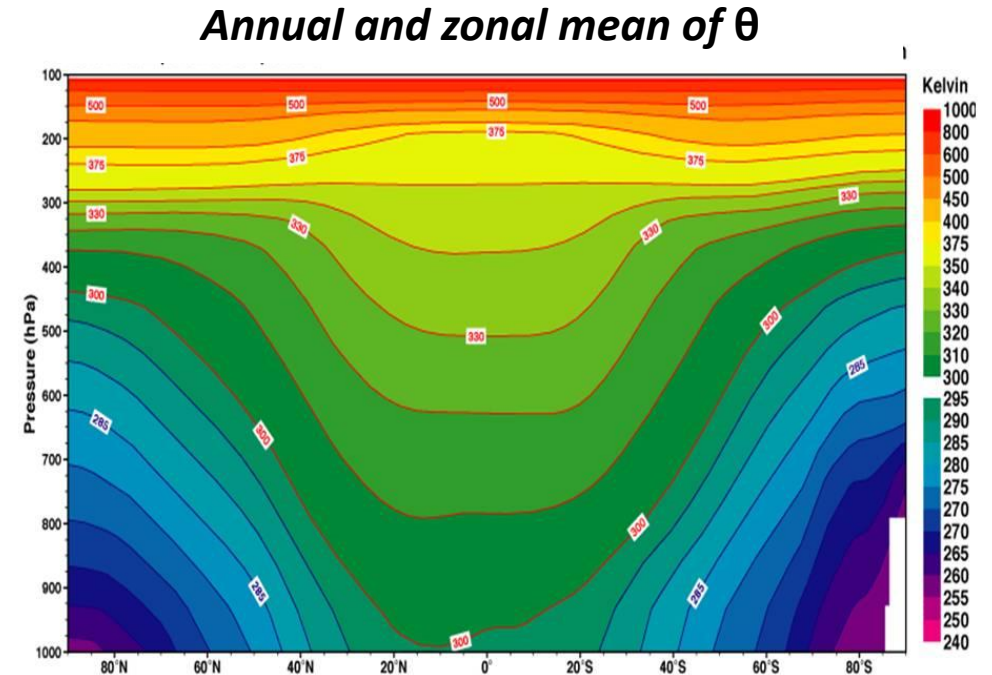
$$f \bar{u} v_z' - f \bar{u}_z v' + w' N^2 = Q.$$

Zonal advection of heat
Meridional advection of heat
Vertical advection of heat

# Basic theory: Hoskins and Karoly (1981)

- If vertical advection of heat dominates, then:

$$v' \simeq fw' / \beta H_Q = fQ / \beta N^2 H_Q$$



$$f\bar{u}v'_z$$

Zonal advection  
of heat

$$-f\bar{u}_z v'$$

Meridional  
advection of heat

$$+ w' N^2$$

Vertical advection  
of heat

$$= Q.$$

# Basic theory: Hoskins and Karoly (1981)

- Key assumption: mechanism with smallest  $v'$  will dominate (this is a thermodynamic argument as the energy source for the motion is heating and this must somehow be converted to kinetic energy)

(1)  $v' \simeq QH_Q / f\bar{u}$  (if zonal adv. dominates)

(2)  $v' \simeq Q / f\bar{u}_z = QH_u / f\bar{u}$  (if meridional adv. dominates)

(3)  $v' \simeq fw' / \beta H_Q = fQ / \beta N^2 H_Q$  (if vertical adv. dominates)

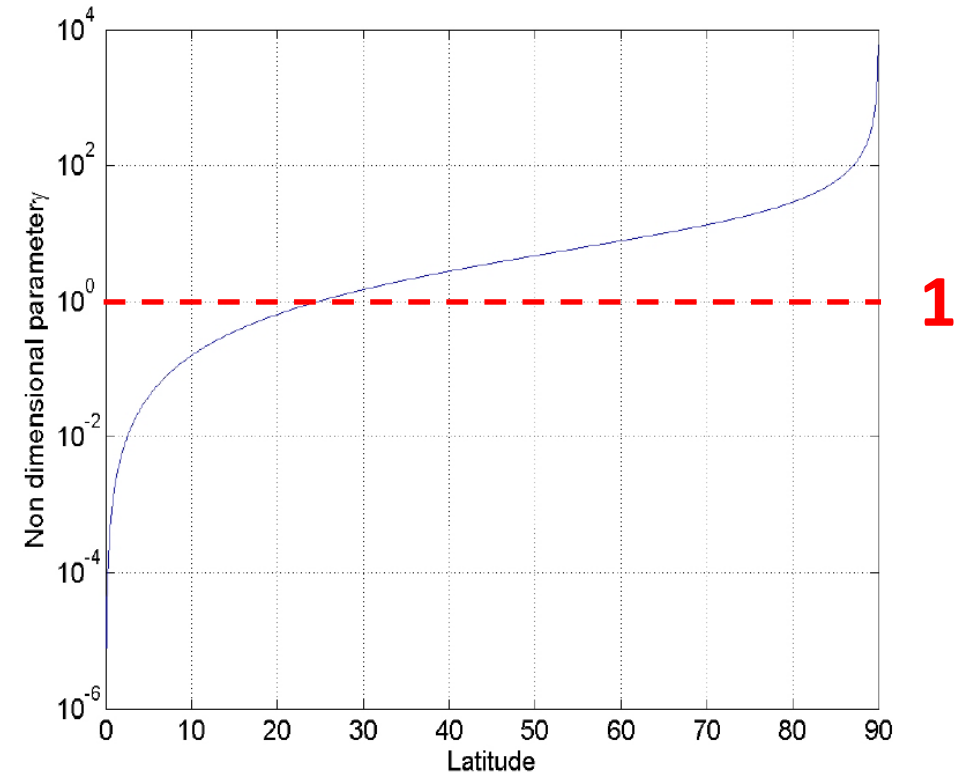
# Basic theory: Hoskins and Karoly (1981)

- The ratio of (3) to (1) or (2) is a non dimensional number:

$$\gamma = f^2 \bar{u} / (\beta N^2 H_Q H)$$

where  $H = \min(H_u, H_Q)$

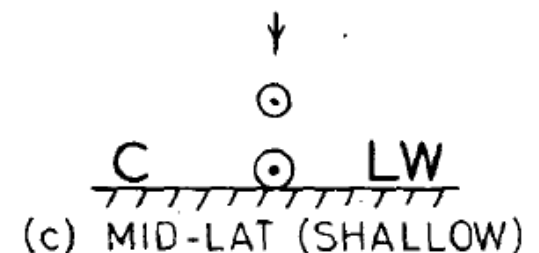
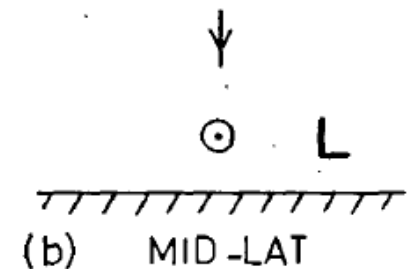
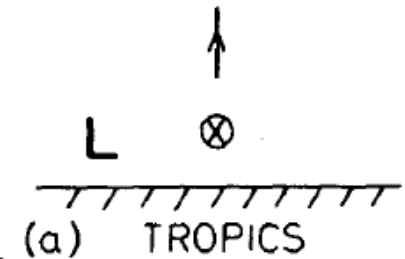
- $\gamma \gg 1$  in midlatitudes (hor. adv. wins)
- $\gamma \ll 1$  in Tropics (vert. adv. wins)



$$H_Q = 6\text{km}, H_u = 3\text{km}, N = 10^{-2}\text{s}^{-1} \text{ and } \bar{u} = 10\text{ms}^{-1}$$

# Basic theory: Hoskins and Karoly (1981)

- $\gamma \ll 1$  in Tropics (vert. adv. wins): upward motion is in phase with the deep heat source. Sverdrup balance requires this to have poleward motion below and thus a low pressure to the west at low levels
- $\gamma \gg 1$  in midlatitudes: if deep heat source then meridional adv. wins at low levels and a low pressure is found to the east of the heat source. This implies sinking motion to accommodate Sverdrup balance.
- $\gamma \gg 1$  in midlatitudes: if shallow heat source then zonal adv. wins at low levels and a cold/warm dipole is found across the source. Sinking motion is again produced.



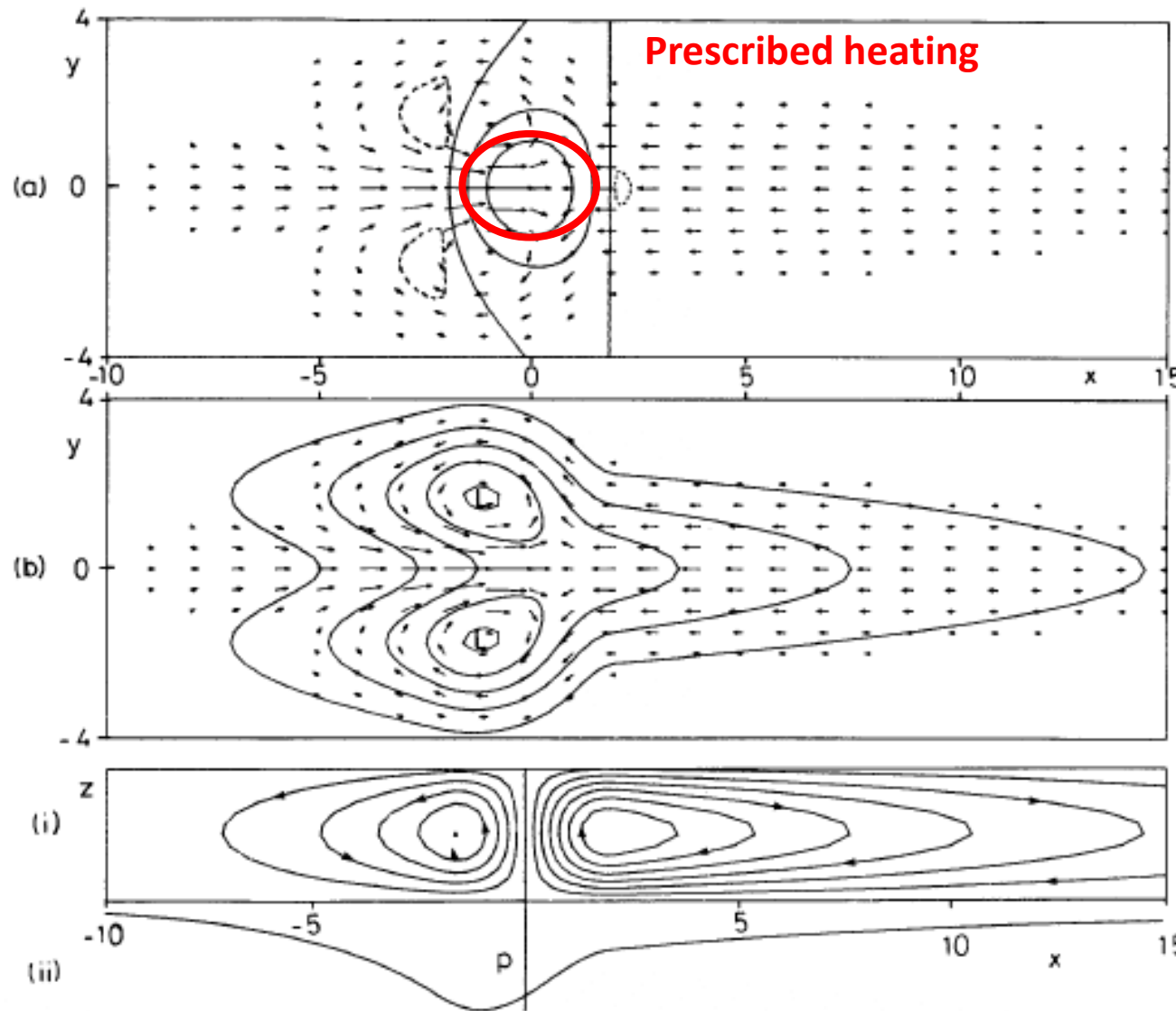


# “Gill’s response” to heating (1980)

Surface wind and vertical motion at midlevel

Surface pressure and winds

Walker cell (longitude-height plane)



Prescribed heating

Figure 1. Solution for heating symmetric about the equator in the region  $|x| < 2$  for decay factor  $\epsilon = 0.1$ .

(a) Contours of vertical velocity  $w$  (solid contours are 0, 0.3, 0.6, broken contour is -0.1) superimposed on the velocity field for the lower layer. The field is dominated by the upward motion in the heating region where it has approximately the same shape as the heating function. Elsewhere there is subsidence with the same pattern as the pressure field.

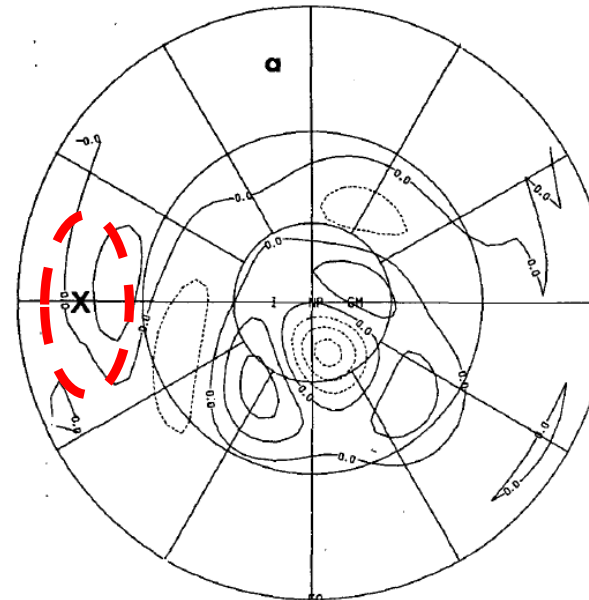
(b) Contours of perturbation pressure  $p$  (contour interval 0.3) which is everywhere negative. There is a trough at the equator in the easterly regime to the east of the forcing region. On the other hand, the pressure in the westerlies to the west of the forcing region, though depressed, is high relative to its value off the equator. Two cyclones are found on the north-west and south-west flanks of the forcing region.

(c) The meridionally integrated flow showing (i) stream function contours, and (ii) perturbation pressure. Note the rising motion in the heating region (where there is a trough) and subsidence elsewhere. The circulation in the right-hand (Walker) cell is five times that in each of the Hadley cells shown in (c).

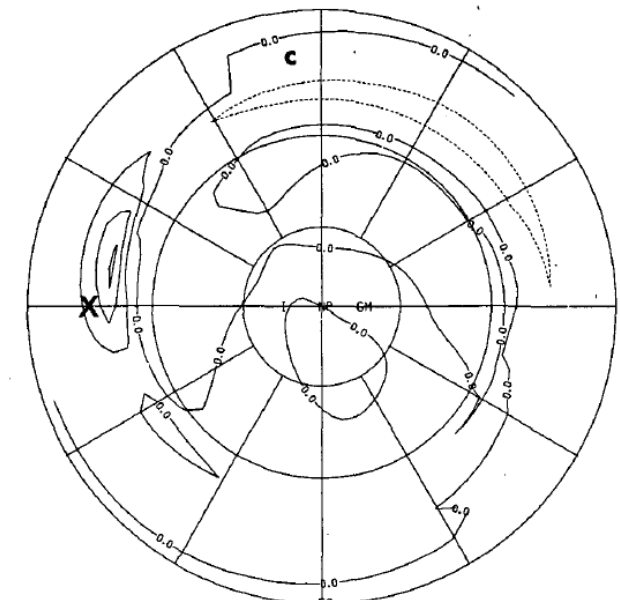
# Hendon & Hartmann's experiments (1982)

- Response to a **deep heat source** (60 deg lon X 30 deg lat, vertically averaged heating of  $350\text{Wm}^{-2}$ ) **centered at 15N**
- Upward motion balances the heating
- Low pressure west of the source at low levels
- Wave train propagating northeastward is generated at upper levels

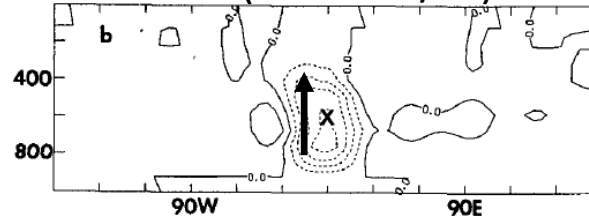
Z at 310hPa (ci=20m)



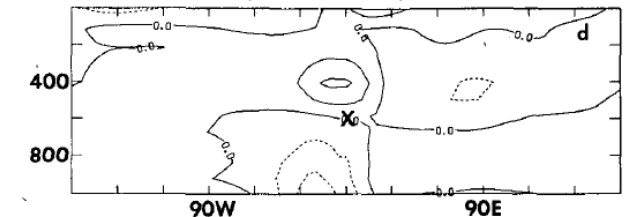
T at 928hPa (ci=1K)



$\omega$  at 18N (ci = 1mb/hr)



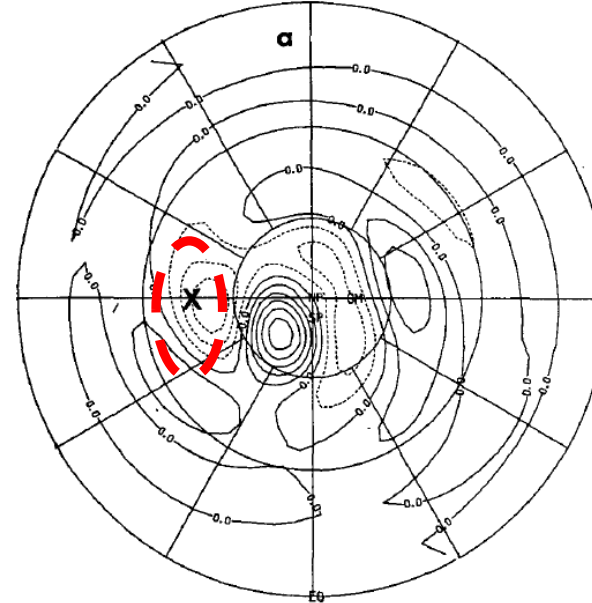
Z at 18N (ci=20m)



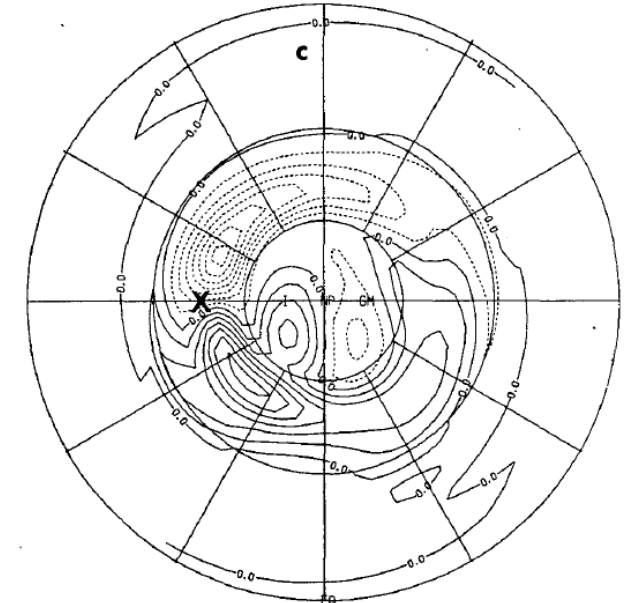
# Hendon & Hartmann's experiments (1982)

- Response to a **shallow heat source** (60 deg lon X 30 deg lat, vertically averaged heating of  $350\text{Wm}^{-2}$ ) **centered at 46N**
- Downward motion over the source & horizontal advection balances the heating
- Strong low pressure east of the source at low levels
- Strong remote response (anticyclone) generated at upper levels

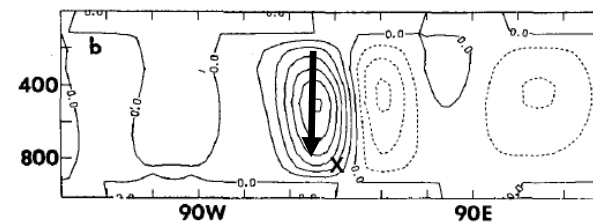
Z at 310hPa (ci=40m)



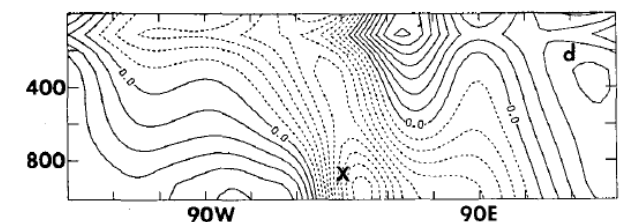
T at 928hPa (ci=1K)



$\omega$  at 46N (ci = 0.2mb/hr)



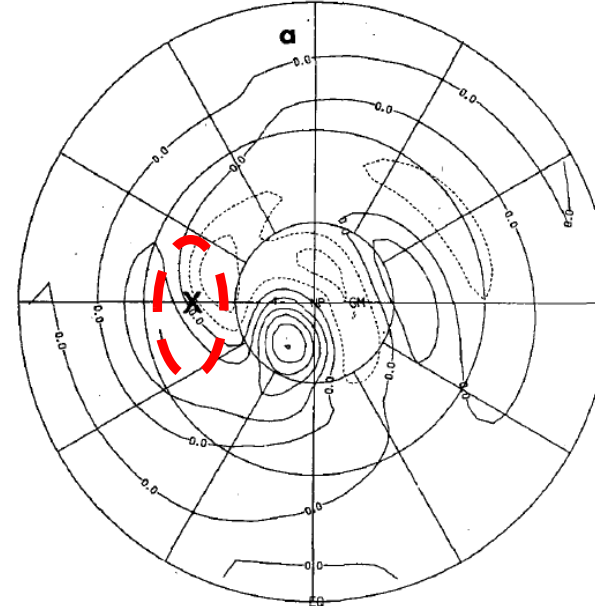
Z at 46N (ci=20m)



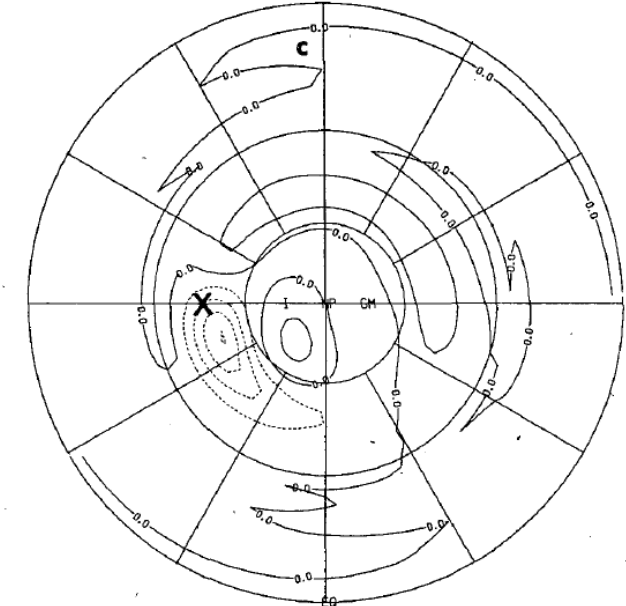
# Hendon & Hartmann's experiments (1982)

- Response to a **deep heat source** (60 deg lon X 30 deg lat, vertically averaged heating of  $350\text{Wm}^{-2}$ ) **centered at 46N**
- Upward and equatorward motion balances the heating & a cold anomaly is produced(!)
- Low pressure east of the source at low levels
- Split wave train is generated at upper levels

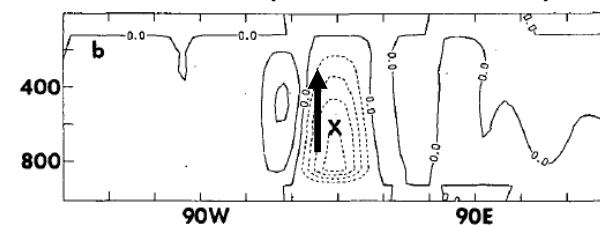
Z at 310hPa (ci=20m)



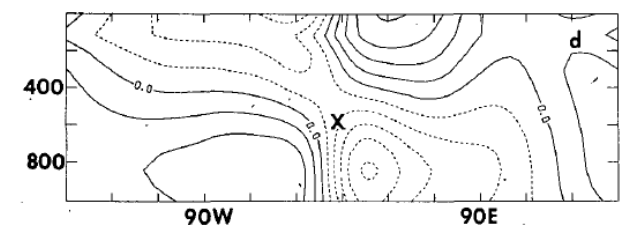
T at 928hPa (ci=1K)



$\omega$  at 46N (ci = 0.2mb/hr)



Z at 46N (ci=20m)



# Challenge...

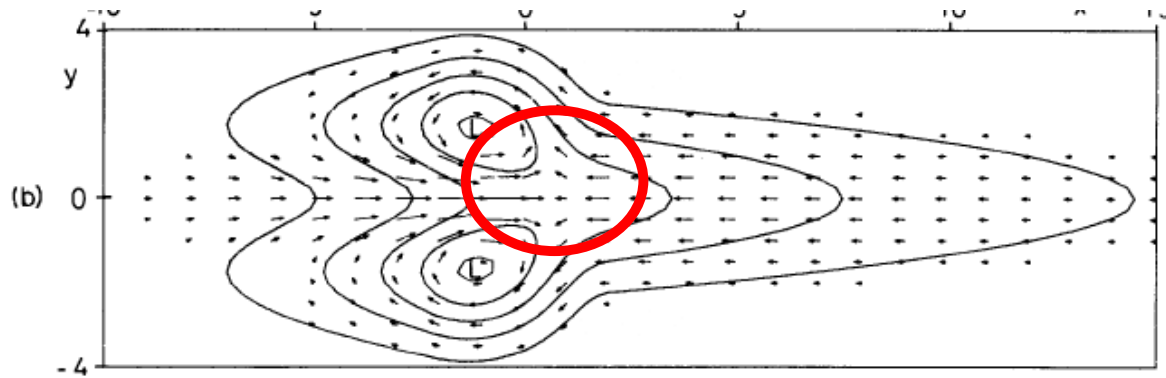
- Use the previous knowledge to compare to more realistic experiments and observations
- Reminder:

$$\langle Q_{app} \rangle = \langle Q_{diab} \rangle - \nabla \cdot \langle v^* \theta^* \rangle$$

Call this  $\langle Q_{fast} \rangle$  (either subgrid scale or high frequency)

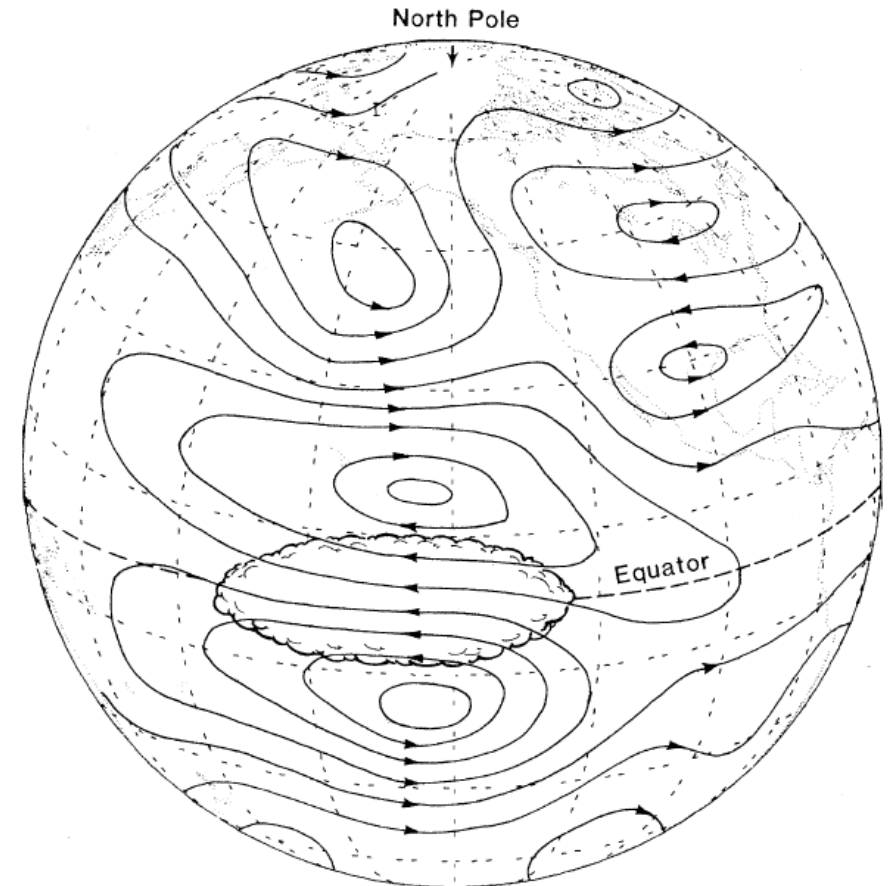
# Gill's response in observations

- Upper level pressure field is the negative of the surface one in Gill's solution



Prescribed heating anomaly

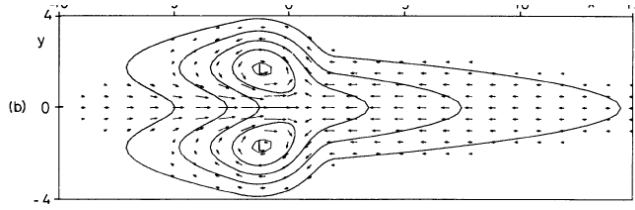
Upper level circulation at the peak of the  
1982-83 El Nino



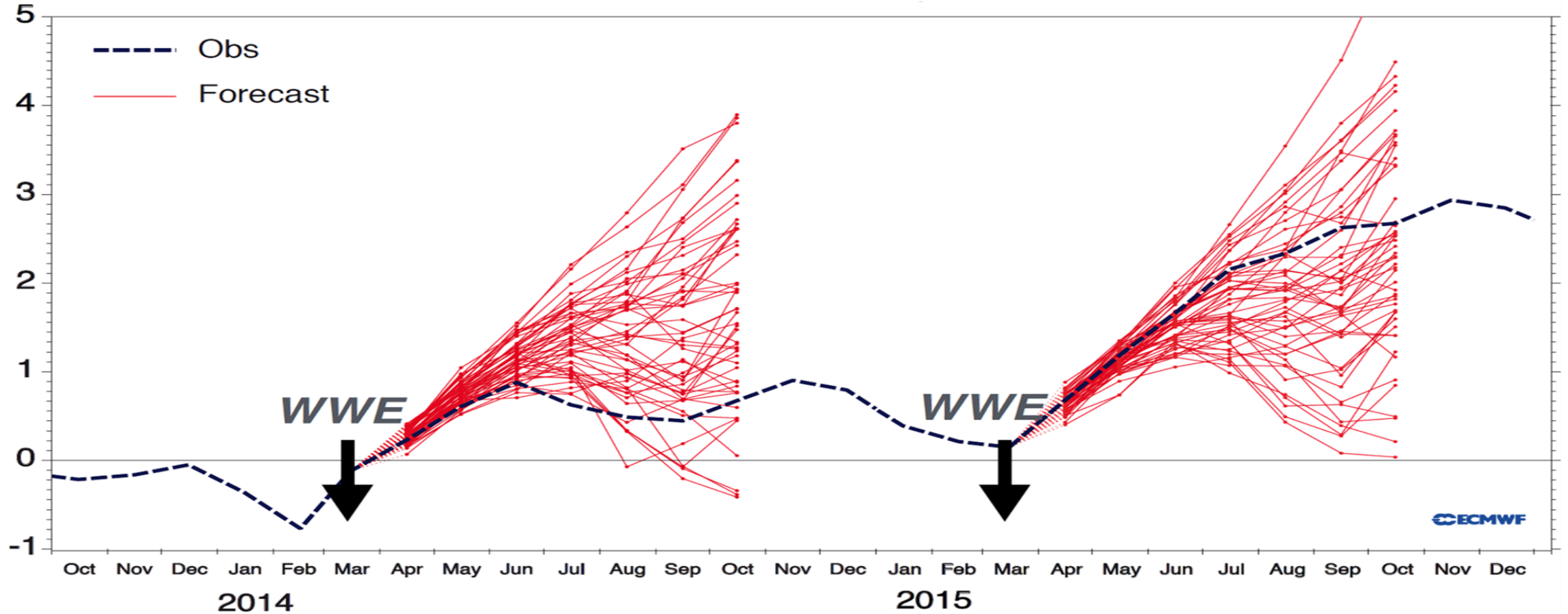
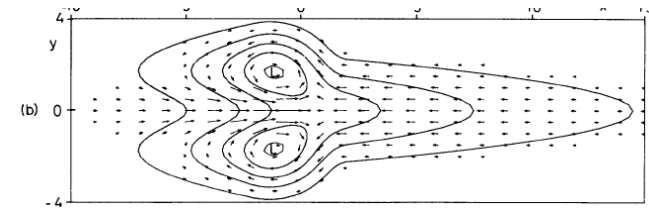
Rasmusson and  
Wallace (1983)

# Predictive skill in the Tropics: “La Nada 2014”

**OFF!**

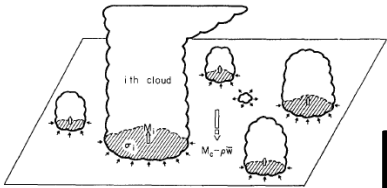


**ON!**



(slide courtesy of J. Vialard)

See McPhaden (2015)



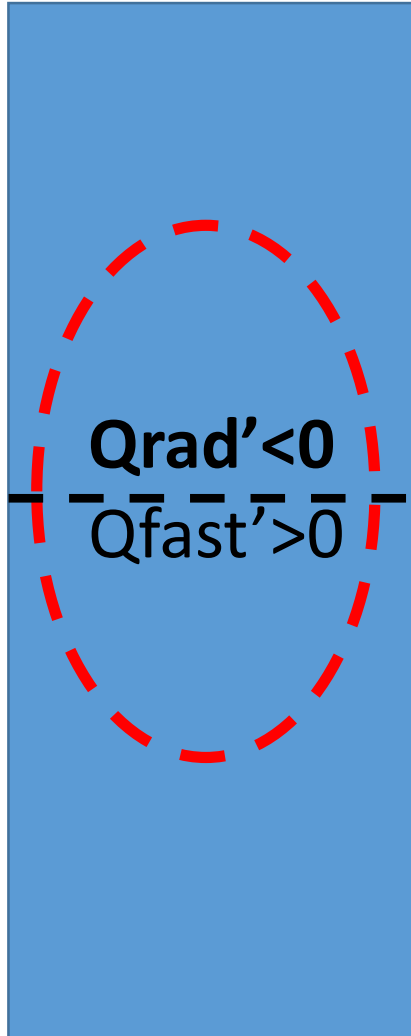
$$\langle Q_{app} \rangle \approx \langle Q_{rad} \rangle + \langle Q_{sen} \rangle + M_c \frac{\partial \langle \theta \rangle}{\partial z} - l_v e$$

La Nada

El Nino

Tropopause

**H**

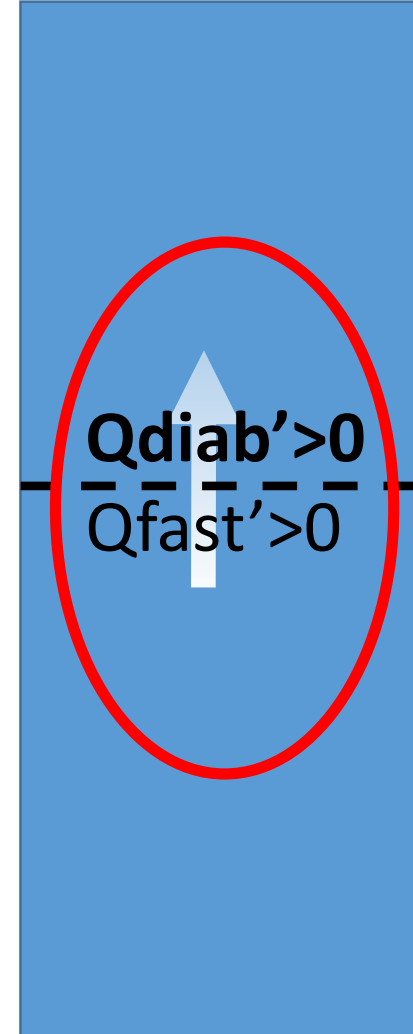


**Qapp' = 0**

**Qrad' < 0**

**Qfast' > 0**

Mid-level



**Qapp' > 0**

**Qdiab' > 0**

**Qfast' > 0**

Low-level

**L**

Warmer ocean

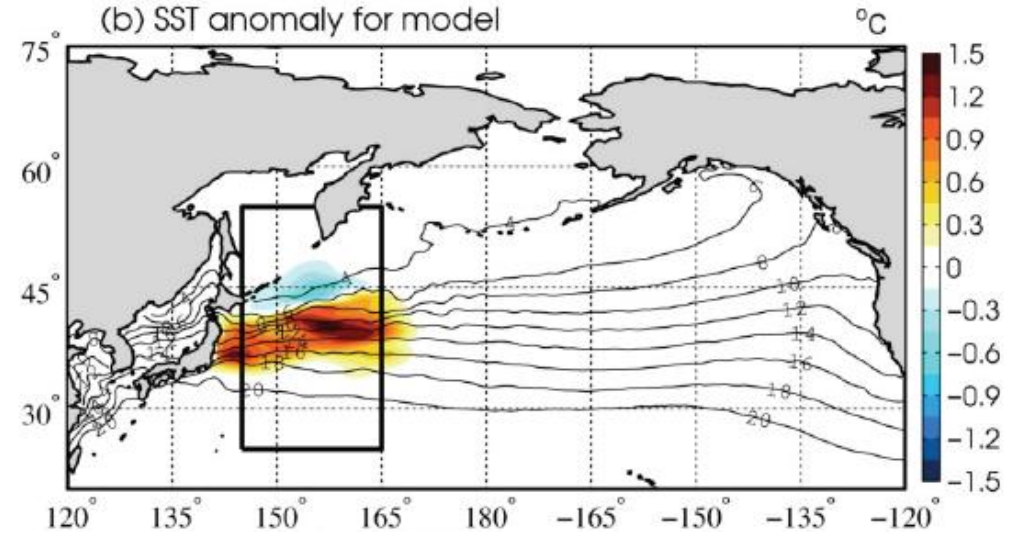
Warmer ocean



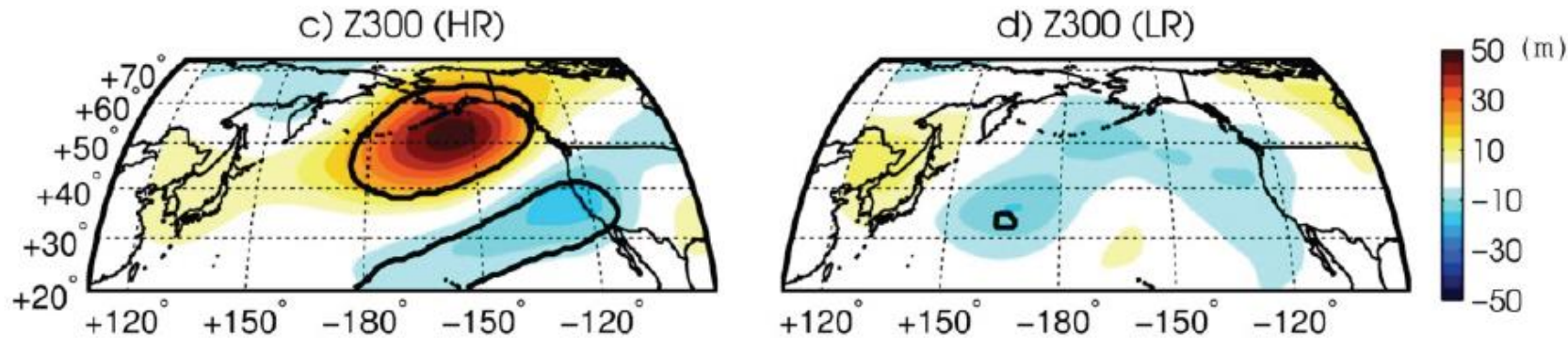
# The Smirnov et al. (2015) experiments

- Comparison of the response of an AGCM to an SST anomaly at two different resolution (~high and low res)
- A very similar **diabatic heating** is produced with two completely different circulation responses!

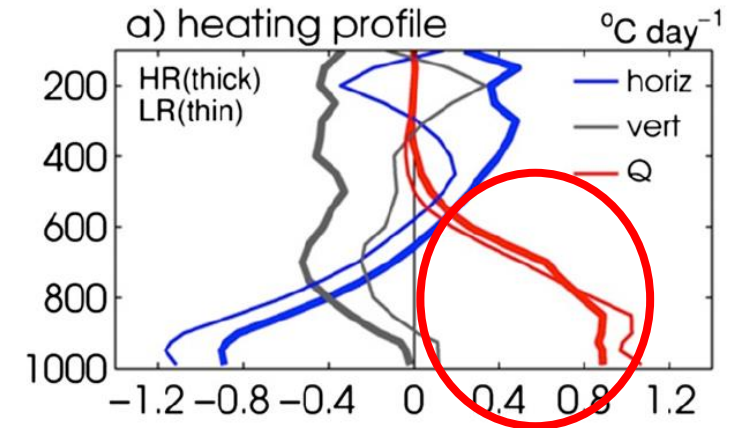
HR = ¼ deg LR = 1 deg



Upper level height anomalies (300hPa)



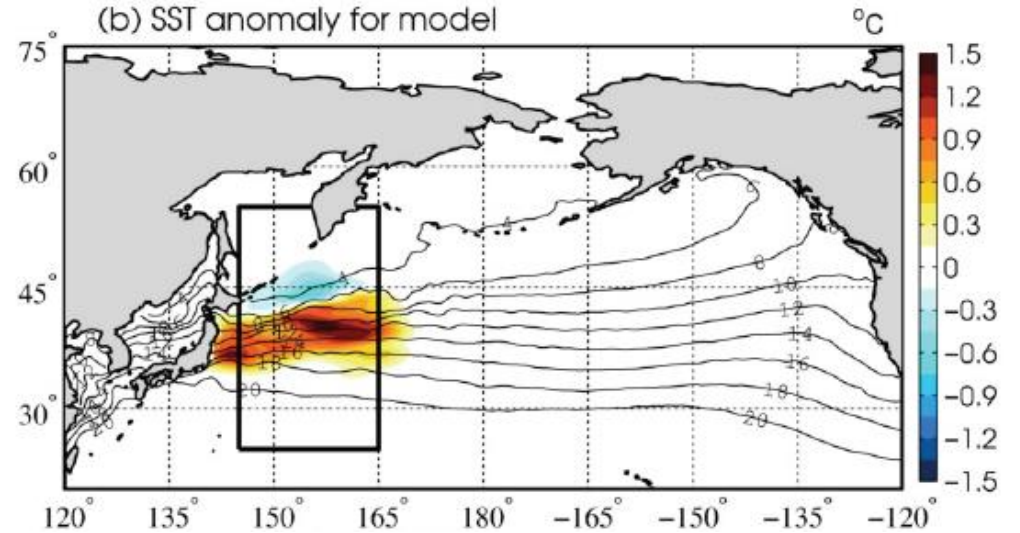
Heat budget components averaged over the box (35-43N)



# ...the “Quantum Café”

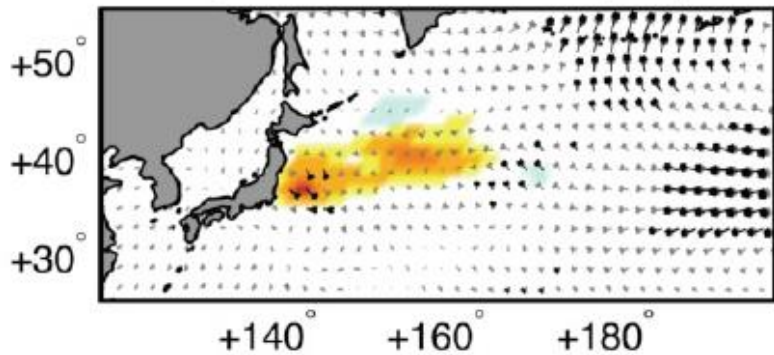
- Comparison of the response of an AGCM to an SST anomaly at two different resolution (~high and low res)
- Completely different responses despite the same Qdiab

HR = ¼ deg LR = 1 deg

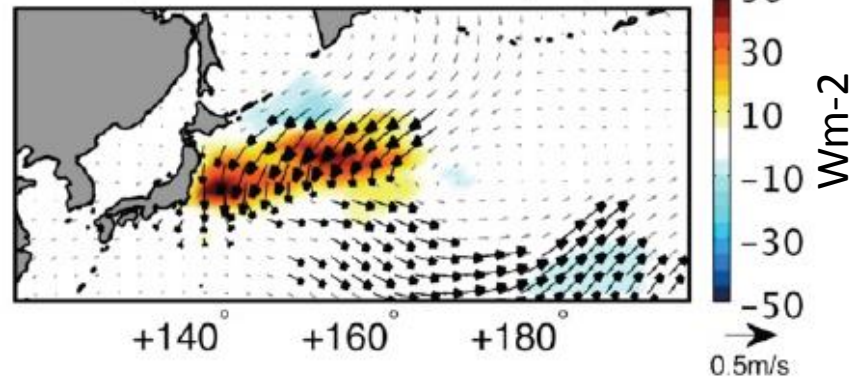


## Surface winds and turbulent heat flux anomalies

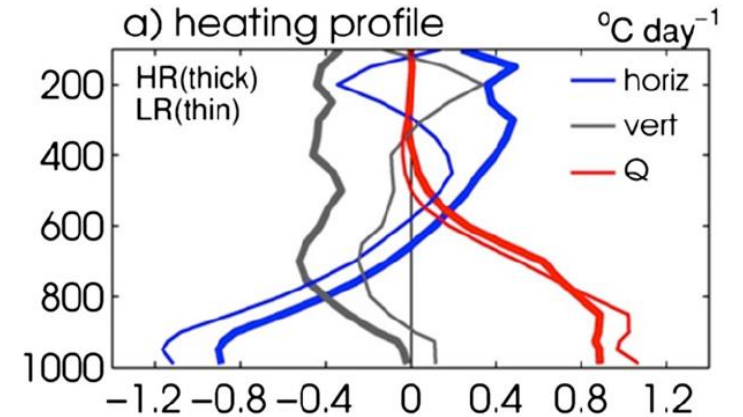
a) THF, 950mb wind (HR)



b) THF, 950mb wind (LR)



## Heat budget components averaged over the box (35-43N)

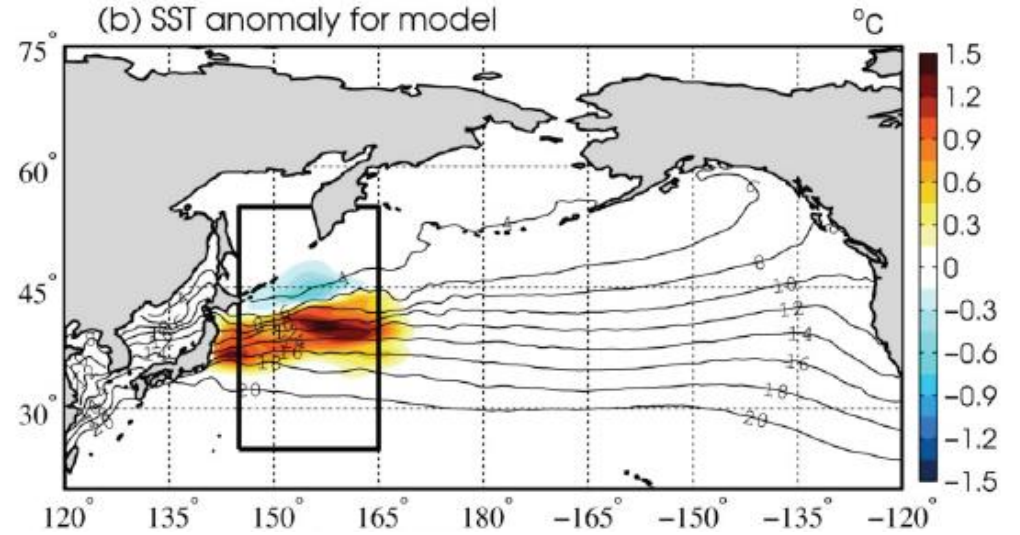


Smirnov et al. (2015)

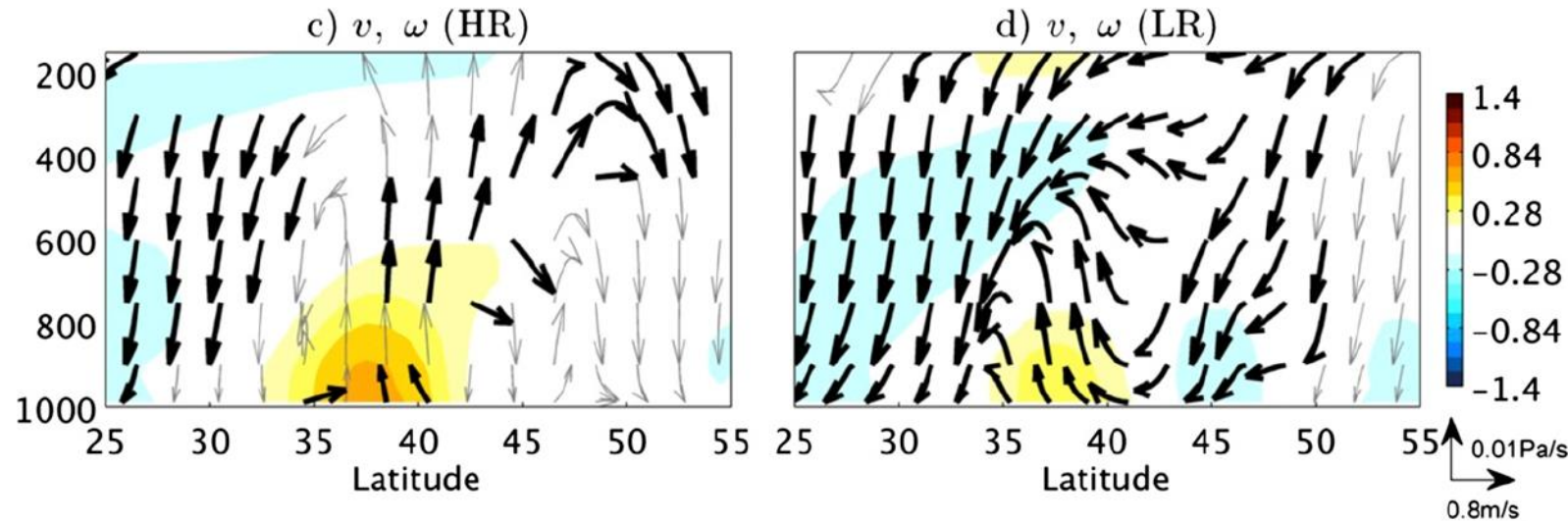
# ...the “Quantum Café”

- Comparison of the response of an AGCM to an SST anomaly at two different resolution (~high and low res)
- Completely different responses despite the same Qdiab

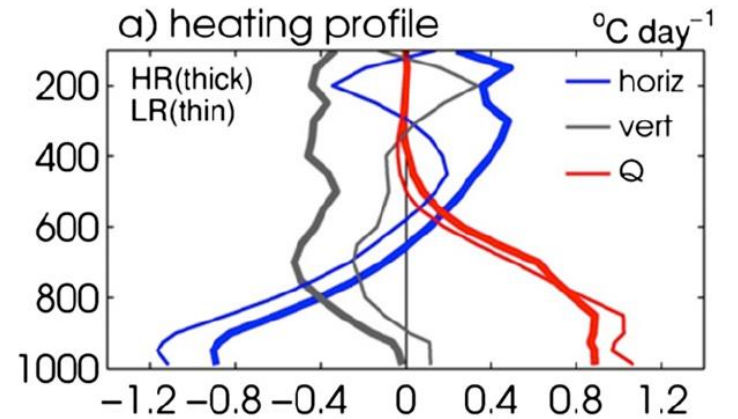
HR = ¼ deg LR = 1 deg



Zonally averaged meridional circulation in the box (color = moist  $\theta$  perturbation)



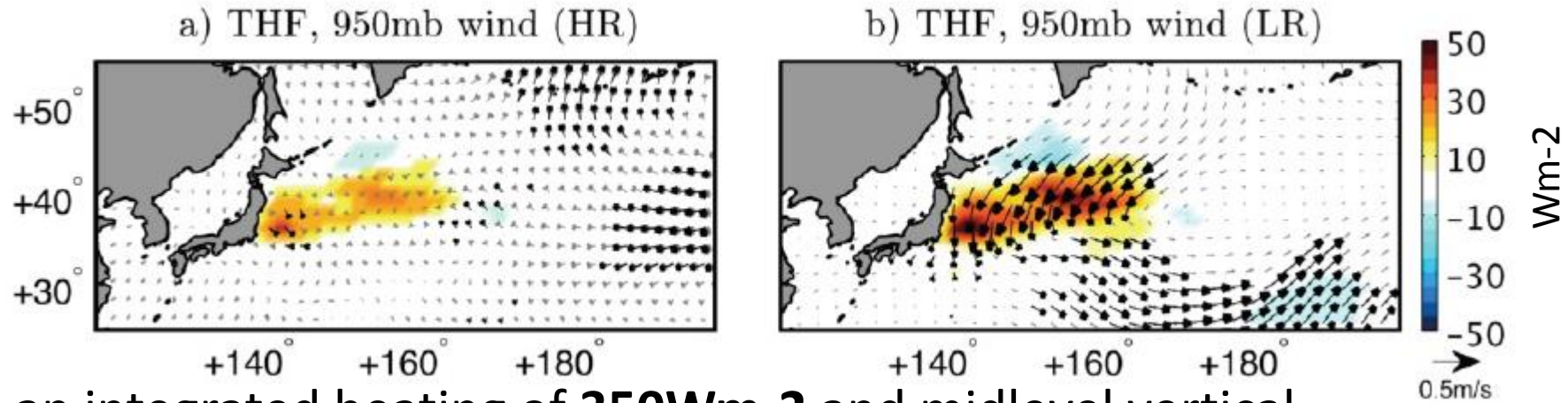
Heat budget components averaged over the box (35-43N)



Smirnov et al. (2015)

# Numbers

## Surface turbulent heat flux anomaly (color) and surface wind vectors



- Hendon & Hartmann had an integrated heating of **350Wm<sup>-2</sup>** and midlevel vertical velocities of:

$$\omega = -4 \text{ mb/hr} = -11.2 \times 0.01 \text{ Pa/s} \quad (\text{deep heating at } 15\text{N})$$

$$\omega = -0.8 \text{ mb/hr} = -2.2 \times 0.01 \text{ Pa/s} \quad (\text{deep heating at } 46\text{N})$$

$$\omega = +1.2 \text{ mb/hr} = +3.4 \times 0.01 \text{ Pa/s} \quad (\text{shallow heating at } 46\text{N})$$

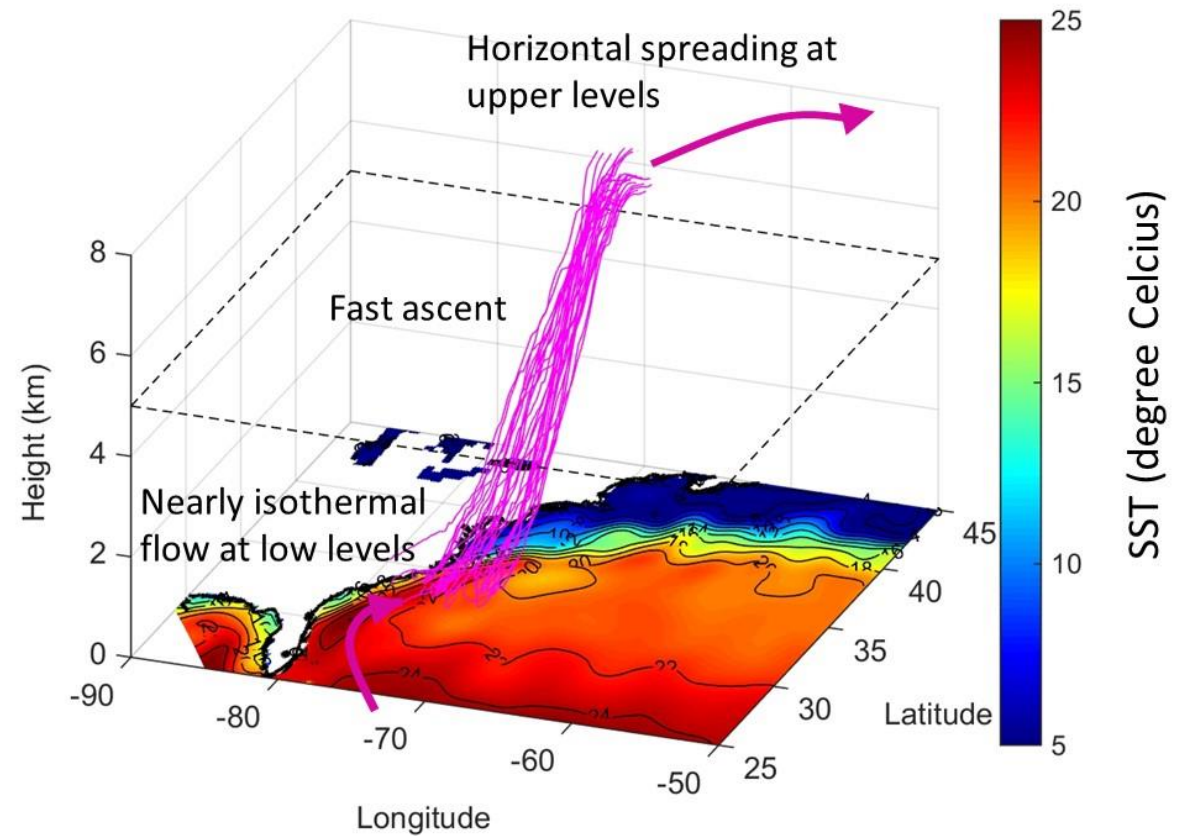
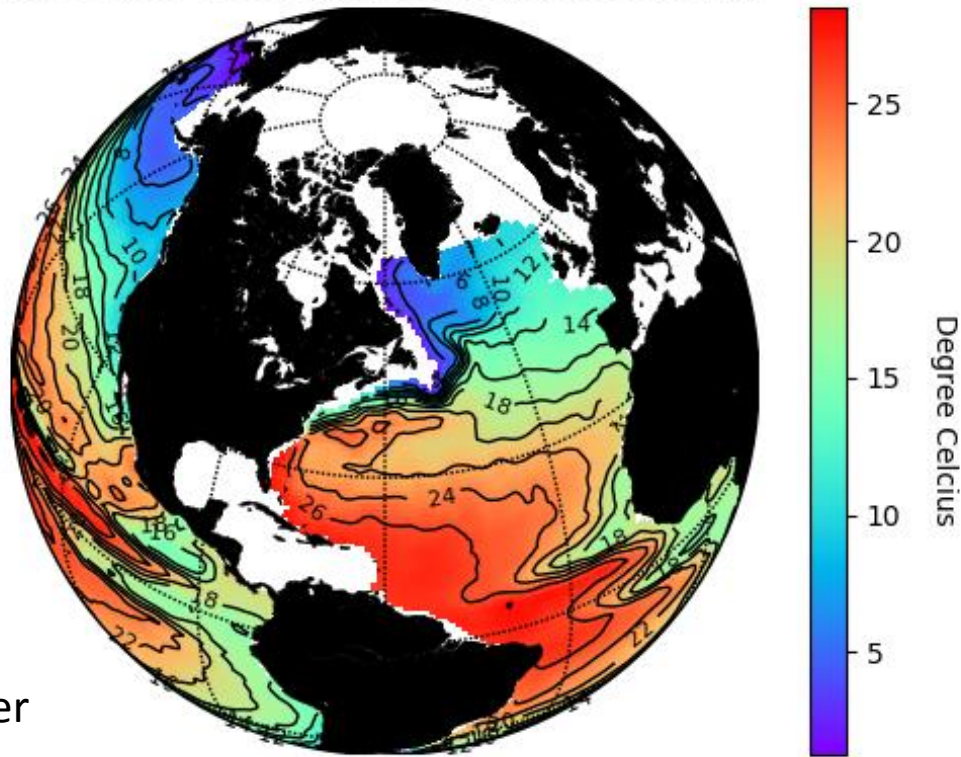
- Smirnov et al. produce, for a surface heat flux anomaly of **20Wm<sup>-2</sup>**, a midlevel vertical velocity of:

$$\omega = -0.01 \text{ Pa/s} \quad (40\text{N SST anomaly in HR})$$

Thus the HR experiment generates midlevel upward motion of similar magnitude as subtropical forcing

# Ascent in weather fronts is sensitive to the Gulf Stream (Sheldon et al., 2017)

ARGO (2004-2015 August mean) at 60.0 dbar



Remember Bob's talk yesterday!

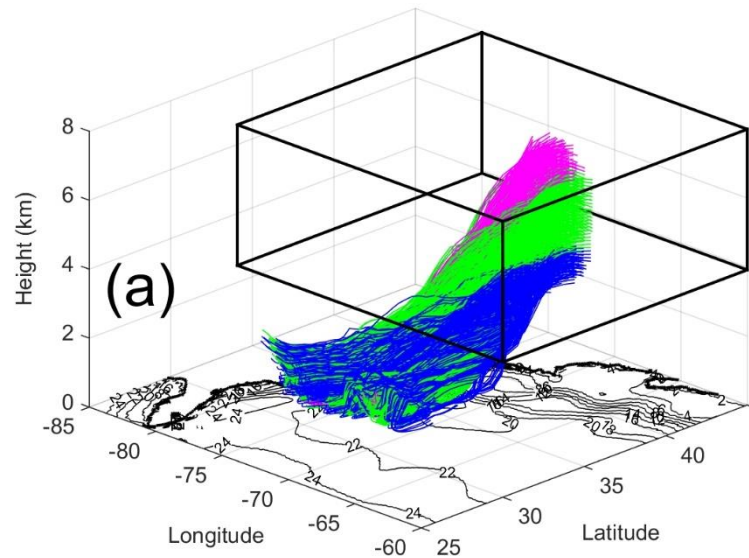
# Ascent in weather fronts is sensitive to the Gulf Stream (Sheldon et al., 2017)

**CNTL**

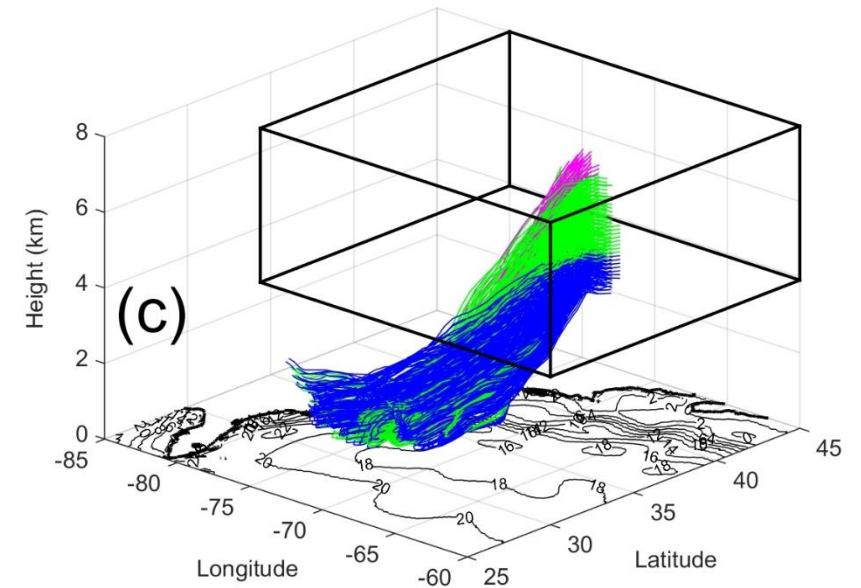
$z_i > 7\text{km}$

$5\text{km} < z_i < 7\text{km}$

$z_i < 5\text{km}$

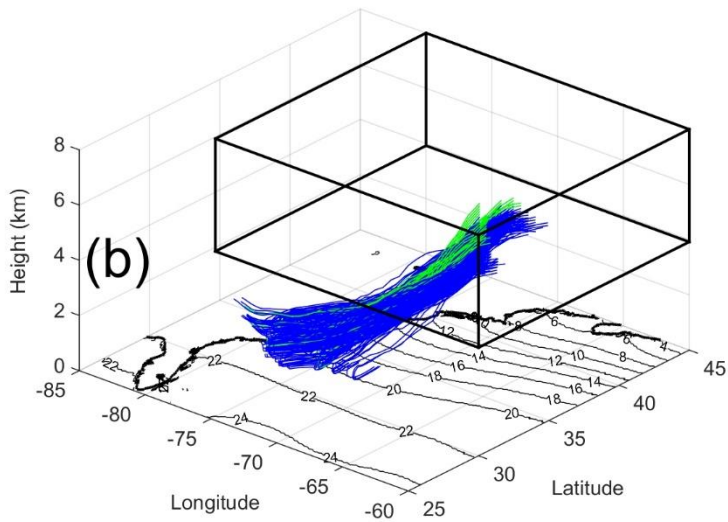


**COOL**



**SMTH**

Initial release volume



Back trajectories  
originating from  
low levels in 12km  
resolution runs

# Ascent in weather fronts is sensitive to the Gulf Stream (Sheldon et al, 2017)

**CNTL**

$z_i > 7\text{km}$

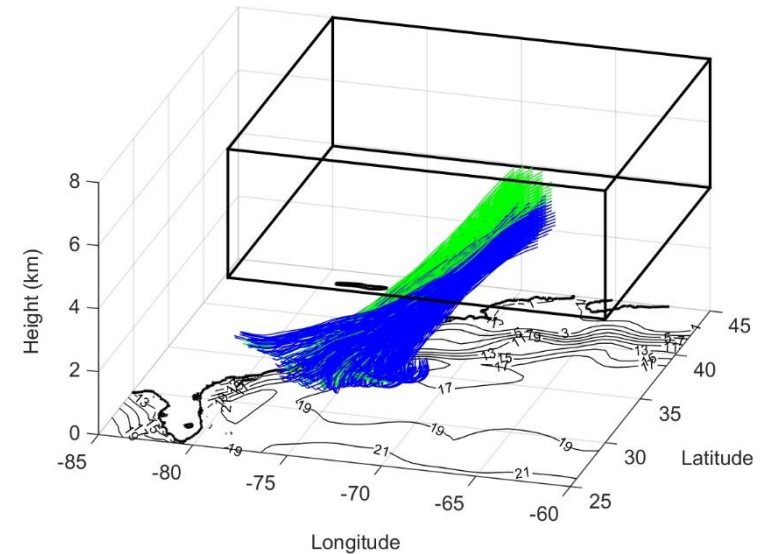
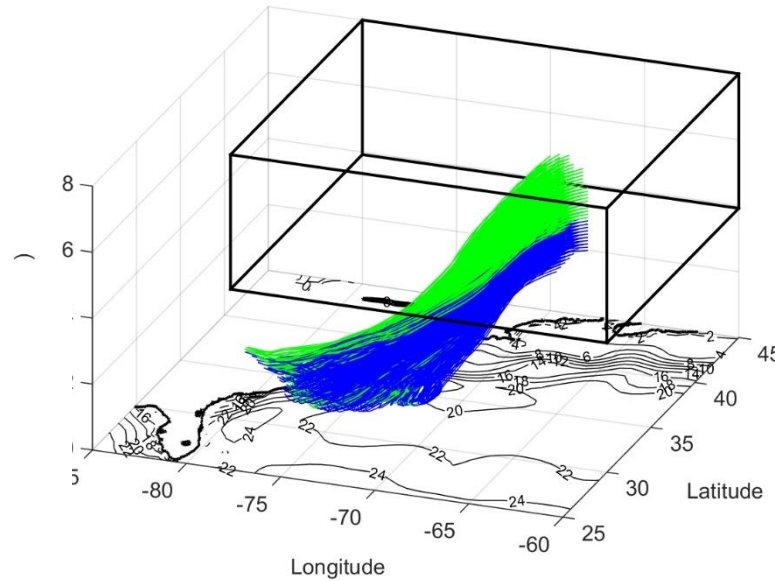
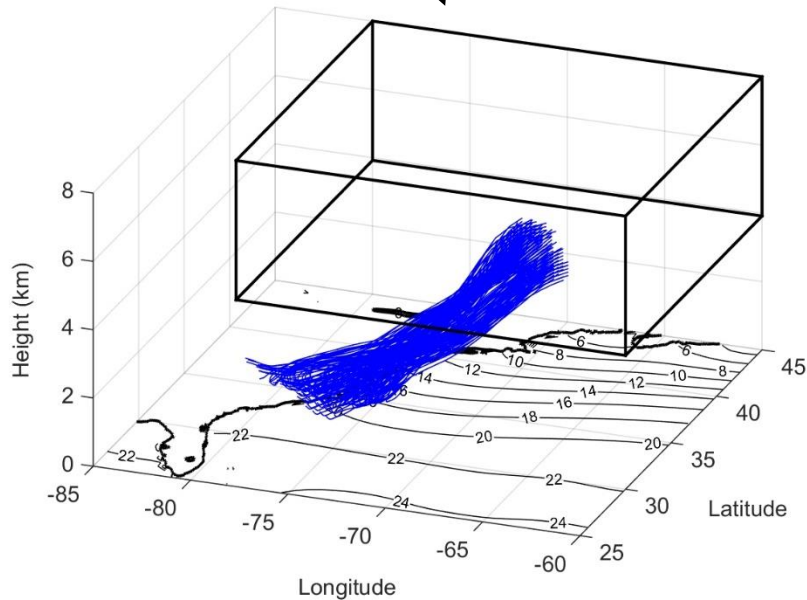
$5\text{km} < z_i < 7\text{km}$

$z_i < 5\text{km}$

**COOL**

**SMTH**

Initial release volume



Back trajectories originating from low levels in 40km resolution runs

# Summary

- The observational record shows well defined “patterns” of co-variability between the ocean and atmosphere on monthly, interannual and possibly decadal timescales. There is a rich range of behaviour between basins in terms of temporal signatures and timescales.
- The standard theory of thermal forcing provides insight into how a warmer/colder upper ocean affects wind and temperature distribution but one must acknowledge the complexity of the link SST → diabatic heating
- There is suggestion that the midlatitude oceanic forcing increases with spatial resolution and might become comparable in magnitude to the low latitude oceanic forcing